Universität Zürich[UZH]

Department of Geography

Development, validation and comparison of a high-performance liquid chromatography (HPLC) method to quantify calcium oxalate (CaOx) in the plant-soil system

ESS 511 Master's Thesis

Author: Grittje Hoppe, 18-733-808

Supervised by: PD Dr. Guido Lars Bruno Wiesenberg, Dr. Mike C. Rowley

Faculty representative: PD Dr. Guido Lars Bruno Wiesenberg

25.04.2025

Abstract

Climate change is a major challenge of this century. Besides a reduction of greenhouse gas emissions, especially carbon dioxide (CO_2), the removal and storage of atmospheric CO_2 (CO_2^{atm}) is essential. One option is the sequestration of carbon (C) as soil organic carbon (SOC) or soil inorganic carbon (SIC), such as calcium carbonate ($CaCO_3$). However, SOC acts as a short-term C sink, while SIC provides long-term storage, which is more effective. The oxalate-carbonate pathway (OCP) efficiently transfers CO_2^{atm} into the geological reservoir as $CaCO_3$ by the catabolisation of calcium oxalate (CaOx). Detection and quantification of CaOx is thus an important part for a thorough investigation of the OCP, its associated species and identification of long-term C sinks. Although a commercial enzymatic oxalate kit (EOK) is typically used, it suffers from low sensitivity, especially in soil samples adjacent to an oxalogenic species with low CaOx concentrations and complex matrices, and the analysis is both costly and time-consuming. Therefore, this study developed a new approach to quantify CaOx in plant and soil samples more precisely.

The novel method involves a quantification with high-performance liquid chromatography (HPLC), which is widely used, has a straightforward method development, is less costly and more precise than the EOK. The optimal HPLC settings involve a C_{18} column at 8 °C, 400 mM phosphoric acid (H_3PO_4) at a flow rate of 0.4 mL/min. Furthermore, the established single step HCl extraction procedure was optimised and replaced by a multi-step extraction procedure based on H_3PO_4 to increase extraction efficiency. By analysing soil and plant samples of an oxalogenic *Ficus* species, both methods were validated and compared based on the criteria, linearity, accuracy, repeatability, applicability and costs.

The new procedure was able to quantify CaOx in plant and soil samples successfully and outperformed the EOK. Compared to the established EOK method, it showed great linearity, higher extraction efficiency and better repeatability at slightly lower costs. Furthermore, time-consuming, error-prone steps could be excluded, such as pH adjustment. However, CaOx in soil samples could not be completely separated from an unknown compound in the HPLC chromatogram, suggesting that the HPLC method still requires some refinement. Additionally, an inexplicable HPLC method shift was noticed during method validation, which led to an increase in the quantified CaOx content of independent samples. Nonetheless, the new method for CaOx quantification provides a powerful tool for investigating active OCPs and thereby identifying long-term C sinks.

List of contents

List of figures

List of tables

List of equations

List of abbreviations

Abbreviation	Connotation
ACN	Acetonitrile
BPCA	Benzene polycarboxylic acid
C	Carbon
Ca	Calcium
$CaCO_3$	Calcium carbonate
CaOx	Calcium oxalate
CH_4	Methane
COV	Coefficient of variation
CO_2	Carbon dioxide
CO_2^{Atm}	Atmospheric carbon dioxide
CO_3^{2-}	Carbonates
C_{org}	Organic carbon
DMAB	3-dimethylaminobenzoic acid
EOK	Enzymatic oxalate kit
Fe	Iron
GC	Gas chromatography
GHG	Greenhouse gas
GMST	Global mean surface temperature
HCl	Hydrochloric acid
HCO_3^-	Bicarbonates
$H_2C_2O_4$	Oxalic acid
H_2O	Water
H_2O_2	Hydrogen peroxide
HPLC	High-performance liquid chromatography
IC	Ion chromatography
IR	Infrared
LC	Liquid chromatograph
M	Mole
MBTH	3-methyl-2-benzothiazolinone hydrazone
MeOH	Methanol
$MgCO_3$	magnesium carbonate
MS	Mass spectrometry
NaOH	Sodium hydroxide
N_2O	Nitrous oxide
OPD	o-phenylenediamine
P	Phosphorus
rpm	Rounds per minute
RSD	Relative standard deviation
SD	Standard deviation
SEM	Scanning electron microscopy
SIC	Soil inorganic carbon

Abbreviation	Connotation
SOC	Soil organic carbon
SOM	Soil organic matter
XRD	X-ray diffraction

1 Introduction

1.1 Climate change

Climate change is one of the most urgent global challenges confronting our society. Numerous papers suggest that more and recurrent extreme weather events, such as heat waves and precipitation extremes, sea level rise and the resulting loss of ecosystems and biodiversity are consequences of a warming climate (e.g., Baldwin et al., 2019; Jaureguiberry et al., 2022; Liu et al., 2022; Myhre et al., 2019). During the history of Earth, surface temperature has constantly been changing, such as a global mean surface temperature fluctuating between 11 °C and 36 °C in the last 485 million years (Judd et al., 2024). However, the present rate of change cannot be compared to the pace of a naturally changing climate (Neukom et al., 2019). Global surface temperature has increased between 2011 and 2020 by around 1.1 °C compared to pre-industrial times (1850-1900; IPCC, 2023). The IPCC further states that the observed warming is unequivocally caused by human activities, mainly by emissions of greenhouse gases (GHG) in the atmosphere. Unsustainable energy use, land-use change, and more consumption are some of the reasons that lead to an increased emission of GHG, mainly carbon dioxide (CO_2), but also methane (CH_4) and nitrous oxide (N_2O). Reducing CO_2 emissions is thus one way to address the climate change problem (Erickson, 2017). Nonetheless, reducing CO_2 emissions is not sufficient to stabilise the global surface temperature and removing CO_2 from the atmosphere and storing it elsewhere is also required (IPCC, 2023).

1.2 Soil organic carbon and soil inorganic carbon

Soil represents the largest reservoir of terrestrial carbon (C) in permanent exchange with the atmosphere (Eswaran et al., 2000; Heimann & Reichstein, 2008; Mohseni & Salar, 2021). It consists of two major forms of C, soil organic carbon (SOC) and soil inorganic carbon (SIC). Those two pools are linked through their joint association with calcium (Ca; Rowley et al., 2018). SOC refers to the carbon fraction of the soil organic matter (SOM) and includes cells of living and dead organisms, plant and animal residues at different stages of decomposition, and tissues of microbes (Lehmann & Kleber, 2015).

It is estimated that approximately 1500 Pg C (Pg = 10^{15} g) are stored as SOC at 1 m depth and 2376 – 2456 Pg C at 2 m depth (Batjes, 1996; Jobbágy & Jackson, 2001). Besides affecting soil fertility positively, leading to increased plant growth and food production, influencing ecosystem stability and resilience and protecting water security, SOC plays a critical role in the C cycle and thus strongly affects atmospheric CO_2

concentrations (Gerke, 2022; Lal, 2004a; Tiessen et al., 1994). Depending on land use, plant biomass input, and climatic conditions, SOC can act as a sink or a source of atmospheric CO_2 (Raza et al., 2024). Agricultural activities are responsible for a loss of about 25 % of SOC from cropped soils – for example, through tillage or drainage of wetlands (Lal, 2004b). On the other hand, it is estimated that through proper management, 0.8 – 1.5 Pg C per year could be removed from the atmosphere by SOC sequestration (Fuss et al., 2018). However, this figure has been debated in the context of the "4 per mille debate", which is an initiative that aims to increase SOC by a rate of 4‰ (0.4 %) relative to the previous year over 20 years through proper land management worldwide. Theoretically, this could lead to a removal of 8.9 Gt CO_2^{atm} per year, an equal amount of the annual CO_2 emissions caused by fossil fuels (L'Initiative internationale "4 pour 1000", 2015). Practically, it is suggested that SOC sequestration is limited by 1 Gt per year (Chabbi et al., 2017). Applying the necessary practices was found to be uneconomic for farmers and could potentially harm global food security (Poulton et al., 2018). Due to these limitations, focusing only on SOC is thus not enough in addressing the climate change problem and including SIC into the discussion is required as well to meet climate change goals (Raza et al., 2024).

SIC refers to the mineral forms of C, involving bicarbonates (HCO_3^-) and carbonates (CO_3^{2-}), such as calcium carbonate ($CaCO_3$) and magnesium carbonate ($MgCO_3$; Batool et al., 2024). The global SIC stock is estimated to be 695 - 930 Pg down to 1 m and 2255 Pg at 2 m depth (Eswaran et al., 2000; Schlesinger, 1982). Once stored in the soil, the residence time of SIC typically lies in the order of 10^2 - 10^6 years (Retallack, 1990). The study Schlesinger (1985) suggests a residence time of 85 k years, which is much longer than the residence time of SOC, typically ranging between 10^1 – 10^3 years for SOC (Prentice et al., 2001). However, it is proposed that despite the long residence time, SIC stocks are not stable and can be affected easily by factors such as land use changes and soil acidification due to intense cultivation or fertilisation practices, which can threaten climate change mitigation action (Zamanian et al., 2021). Despite playing a major role in regulating CO_2^{Atm}, SIC has been largely neglected in soil C research (Raza et al., 2024). Thereby, highlighting a need to further study this important C cycle and the mechanisms governing its loss and formation (Batool et al., 2024). One possible mechanism to transfer CO_2^{atm} efficiently in the SIC reservoir is the oxalate-carbonate pathway (OCP; Cailleau et al., 2004).

1.3 Oxalate-carbonate pathway

The OCP (Fig. 1) is a biogeochemical cycle that sequesters CO_2^{Atm} as $CaCO_3$ in the soil. It starts with the fixation of CO_2^{Atm} by plants (RuBisCo) during photosynthesis, whereby biomass (C_{org}) and then oxalic acid ($H_2C_2O_4$) are formed (Verrecchia, 1990). Some plants can then convert oxalic acid into insoluble calcium oxalate crystals (CaOx, CaC_2O_4.n H2O; Franceschi & Nakata, 2005). By decomposing oxalic acid or oxalate-rich litter, the conversion can also be performed by fungi, which can also shuttle oxalotrophic bacteria through fungal highways (Bravo et al., 2013; Junier et al., 2021). After CaOx crystals are released by exudation or during decomposition (Cailleau et al., 2011; Jayasuriya, 1955), they can be catabolised by oxalotrophic bacteria through two different pathways the glycolate and serine pathway and precipitate as $CaCO_3$ (Sahin, 2003). In summary, during the OCP, one mole (M) is respired and released again as CO_2 while another M is converted to $CaCO_3$ and stored as SIC (Eq. 1; Aragno et al., 2010).

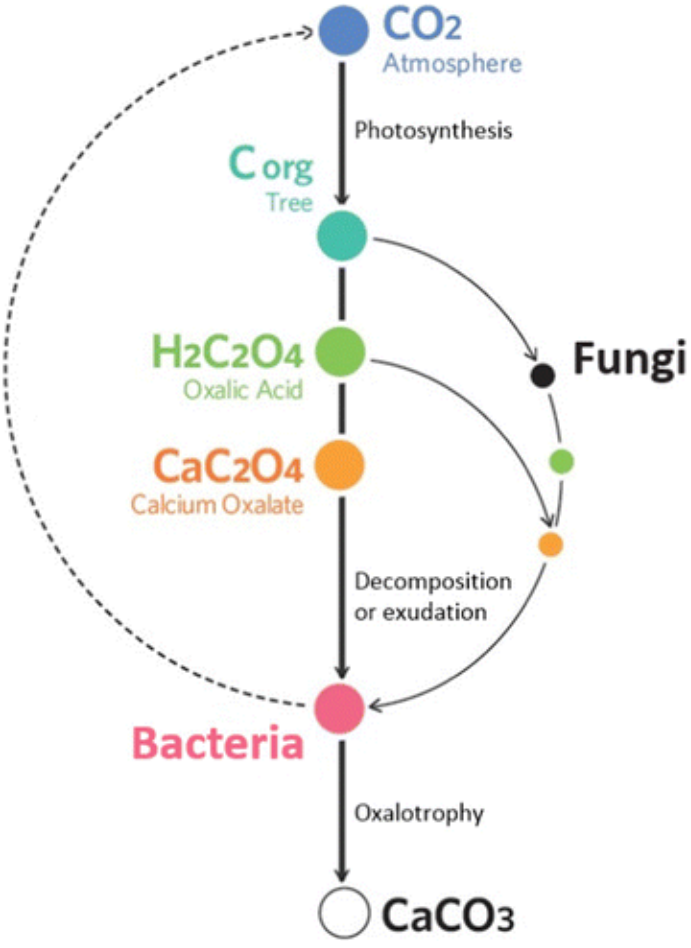

Fig. 1: Schematic sketch of the OCP (Rowley et al., 2017)

$$CaC_2O_4.n\,H_2O + {}^1/_2\,O_2 \rightarrow CaCO_3 + CO_2 + (n)\,H_2O$$

Eq. 1: Summary of the OCP. Oxidation of CaOx leads to the production of $CaCO_3$, CO_2 and H_2O (Aragno et al., 2010).

If Ca is provided by an external source for SIC formation, e.g., Ca of silicate rocks via dust input, the OCP represents a true C sink and probably plays an important role in regulating CO_2^{Atm} but has largely been understudied (Cailleau et al., 2005, 2014; Verrecchia et al., 2006). Various oxalogenic species have been identified, mainly by using the alkalinisation of acidic soils as a proxy (Braissant et al., 2002; Cailleau et al., 2004, 2014; Monje & Baran, 2002). However, *Brosimum alicastrum Sw*. is a confirmed oxalogenic species in a calcareous soil environment by also looking at CaOx dynamics, which shows the complexity of identifying an active OCP (Rowley et al., 2017). Furthermore, it is one of the few agroforestry species that have been investigated in connection with the OCP. Agroforestry refers to a land-use management system that integrates crops and trees to increase productivity, biodiversity and sustainability (Nair et al., 2022). Thus, focusing on agroforestry species associated with an active OCP is beneficial not only in terms of climate change mitigation by C fixation but providing other ecosystem services.

1.4 Calcium oxalate

CaOx crystals are a key component of the OCP, without which the associated SIC sequestration would not be possible. Their presence thus might act as a proxy for an active OCP. Therefore, the formation and functions will be discussed briefly.

CaOx intracellular biosynthesis requires, besides oxalic acid, a low molecular weight organic acid, and Ca, also other organic materials. Within the CaOx accumulating cell, the crystal idioblast, an unstable supersaturated solution is created from which the CaOx crystals are metabolised (Franceschi & Nakata, 2005). Two main hydration states of CaOx can be found within the crystal idioblast: whewellite, the monohydrate system ($CaC_2O_4.H_2O$) and the dehydrate system, weddellite ($CaC_2O_4.2\,H_2O$; Monje & Baran, 2002). Whewellite is the most common system in plants (Verrecchia et al., 2006). The presence of CaOx has been reported throughout all taxonomic levels of photosynthetic organisms and has several primary and secondary functions (Franceschi & Nakata, 2005). Providing a high-capacity Ca-regulation is the first primary phyto-function. By incorporating Ca into insoluble CaOx crystals (solubility: $K_{ps} = 4 \cdot 10^{-9}$; Braissant et al., 2002), the idioblast acts as a Ca sink. Toxic Ca levels can be reduced by releasing the CaOx crystals (Franceschi & Nakata, 2005; Volk et al., 2002). The second main function of CaOx is the protection from herbivory. CaOx can act as a physical deterrent against larger herbivores (Ruiz et al., 2002) or against larvae as

an injury factor against larvae (Konno et al., 2014). However, it is argued that the protection against herbivory cannot be generalised and provides protection only in particular cases (Paiva, 2021). Besides that, different secondary functions of CaOx have been observed, such as the detoxification of various heavy metals (Nakata, 2003) and an increase in the availability of phosphorus (P) and other nutrients (Cannon et al., 1995).

1.5 Methods for oxalate detection and quantification

Detecting and quantifying oxalate in the plant-soil system is essential for a throughout understanding of the OCP and its impacts on the ecosystem (Cowan et al., 2024). Over the last 40 years, a broad variety of qualitative and quantitative methods have been reported in the literature, showing that each method comes with its advantages and disadvantages, and the most suitable method has to be selected depending on the goal of the study (Misiewicz et al., 2023). Since this thesis is not a literature review on different methods, only the most important and commonly used techniques are discussed briefly to provide a general overview.

Detection methods visualise the internal and overall structure of CaOx crystals and include optical microscopy, scanning electron microscopy (SEM), X-ray diffraction (XRD) and infrared (IR) spectroscopy (Braissant et al., 2004; G. Cailleau et al., 2011; Monje & Baran, 2002; Rojas-Molina et al., 2015; Schmitt et al., 2018).

However, quantifying CaOx instead of solely detecting it allows a deeper insight and better understanding of the involved processes (Cowan et al., 2024). Electrochemical methods are conductivity-based and considered to be the most sensitive quantification technique, and have been applied for soil and plant samples as well as organisms (Kotani et al., 2023; Strobel et al., 2004; Varão Moura et al., 2022). Nonetheless, the method is limited by poor resolution (Misiewicz et al., 2023). Methods involving tandem mass spectrometry (MS), such as liquid chromatography-MS (LC-MS), ion chromatography-MS (IC-MS) and gas chromatography-MS (GC-MS) have shown great sensitivity, selectivity and accuracy for oxalate (Li et al., 2022; Mu et al., 2022; Van Harskamp et al., 2020). However, the approach is costly, further expertise is required for method development, and sample preparation is also time-consuming due to matrix effects or volatising oxalate for GC (Gómez et al., 2022).

Enzymatic methods are reported to quantify CaOx in plant and soil samples effectively (Certini et al., 2000). Due to its easy application, a commercial enzymatic oxalate kit (EOK) is widely used as an enzymatic approach to quantify CaOx in plant and soil samples (Álvarez-Rivera et al., 2021; Cailleau et al., 2014; Rowley et al., 2017). The

kits are based on simple enzymatic reactions and can be summarised with the following two reaction equations in the case of the Biotech Trinity EOK:

$$\text{Oxalate} + O_2 \xrightarrow{\text{Oxalate Oxidase}} 2\,CO_2 + H_2O_2$$

Eq. 2: Step 1 of the enzymatic reaction: Enzymatic oxidation of oxalate by oxalate oxidase, catalysing its breakdown into CO_2 and hydrogen peroxide (H_2O_2).

$$H_2O_2 + \text{MBTH} + \text{DMAB} \xrightarrow{\text{Peroxidase}} \text{Indamine Dye} + H_2O$$

Eq. 3: Step 2 of the enzymatic reaction: Previously produced H_2O_2, 3-methyl-2-benzothiazolinone hydrazone (MBTH), and 3-dimethylaminobenzoic acid (DMAB) produce an indamine dye and H_2O by peroxidase.

In Eq. 2 oxalate is oxidised to CO_2 and hydrogen peroxide (H_2O_2), while in the second step, the resulting H_2O_2 is reacted with 3-methyl-2-benzothiazolinone hydrazone (MBTH) and 3- (dimethylamino) benzoic acid (DMAB) to produce water (H_2O) and an indamine dye (Eq. 3). This type of reaction can also be called peroxidase. The absorbance maximum of the generated indamine dye lies at 590 nm, but this is dependent on the EOK. Since its colour intensity is directly proportional to the oxalate concentration of the sample, the oxalate content can be quantified with the use of standards. However, low oxalate concentrations in a complex sample matrix cannot be quantified accurately due to interferences by other compounds (Hansen et al., 1994; Zuo et al., 2010). Especially for soil samples with a complex matrix and rather low CaOx content, the kit was only used in one study conducted by Álvarez-Rivera et al. (2021) but failed in other cases to accurately quantify CaOx (Rowley et al., 2017). In addition, sample preparation involves pH adjustment, which is time-consuming, and the kits are costly (Sigma-Aldrich Co. LLC, 2023; Trinity Biotech PLC, 2013).

High-performance liquid chromatography (HPLC) is a less commonly used but promising approach in quantifying CaOx (Shen et al., 2021). Compared to the EOKs, it shows a higher sensitivity and selectivity, its application is easier, and it is less costly (Hönow & Hesse, 2002). Relative to very sensitive MS methods, such as LC-MS, HPLC is less costly and less complex in method development and available in the majority of laboratories (Locatelli et al., 2019). Figure 2 depicts a schematic sketch of an HPLC system (Afsarimanesh et al., 2018). Quantification is accomplished by injecting a sample extract into the HPLC system, where a solvent, the mobile phase, is pumped through at high pressure and at a certain flow rate. In the column, the stationary phase, the sample compounds are separated based on their chemical properties and pass through the column faster or slower. Consequently, different retention times are detected and visualised in a chromatogram by peaks (Abdu Hussen, 2022). Due to the various parameters that can be changed, such as solvent, its flow rate or column type, the method can be adapted widely and is a good alternative

to the EOKs. However, a development process is required to tailor the method's parameters towards the inventory of the corresponding laboratory and optimise it.

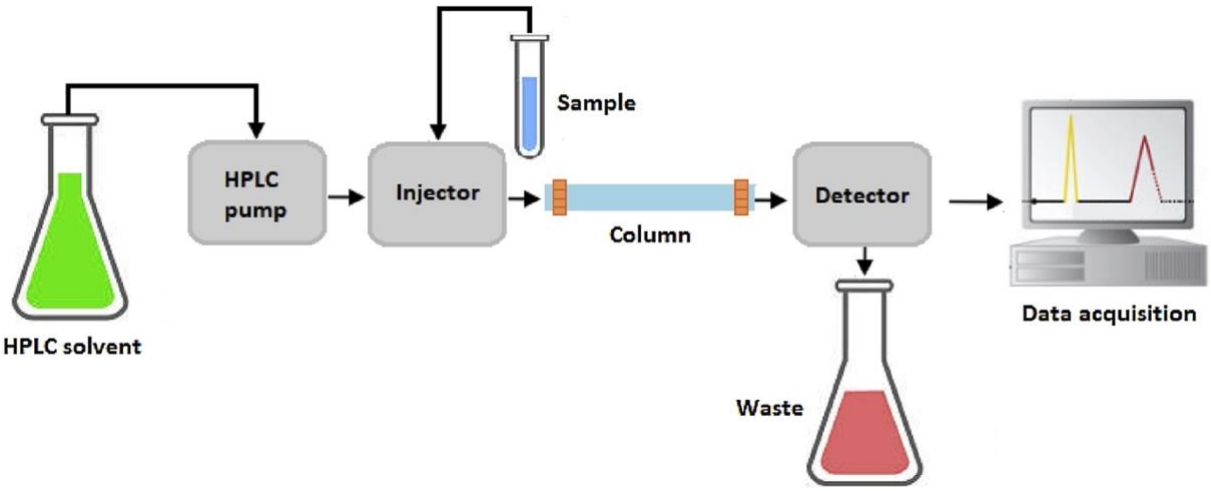

Fig. 2: Schematic sketch of an HPLC system (Afsarimanesh et al., 2018)

1.6 Objectives, research questions and expected results

Given the limited sensitivity of the established EOK method to precisely quantify CaOx in plant and soil samples, there is a critical need for a more reliable and cost-effective approach to identify active OCPs more easily and thereby study long-term C sinks for climate change mitigation. Hence, this thesis aims to address this methodological gap by developing and evaluating a novel HPLC method for accurately quantifying CaOx in the plant-soil system. Specifically, this study is divided into three parts with an objective and a corresponding research question to accomplish this goal.

Part I: Method development

- **Objective 1:** Formulate an HPLC method optimised for CaOx quantification in both plant and soil samples by systematically adjusting chromatographic parameters, such as flow rate, solvent, and column type (parameters are stated in chapter 3.2).
- **Objective 2**: Adapt and optimise the existing extraction procedure to increase the extraction efficiency of CaOx and enhance applicability, while ensuring compatibility with the HPLC method by systematically adapting parameters, such as extraction acid, dilution, and filtration (parameters are stated in chapter 3.1).
- **Research question 1:** What are the optimal settings for an extraction protocol and HPLC procedure to quantify CaOx?

Part II: Method validation

- **Objective 3:** Analyse a test sample set of an oxalogenic species, standards, and spiked samples with the newly developed extraction and HPLC protocol. Use the obtained data to validate both the EOK and HPLC methods in terms of extraction

efficiency, sensitivity, accuracy, and cost-effectiveness (validation criteria and their target value are outlined in chapter 4.1).

- **Research question 2:** How do the newly developed extraction and HPLC methods perform when applied to plant and soil samples of an oxalogenic species, and do they meet the established validation criteria?

Part III: Method comparison

- **Objective 4:** Compare both methods based on the previously validated criteria.
- **Research question 3:** What are the differences in performance between the new method and the established EOK method, and which modifications contribute most significantly to these differences?

Since the research questions are descriptive, no hypotheses were formulated that could be verified by statistical analysis. Instead, it was focused on expected results for parts II and III. It is expected that the new method is capable of analysing plant and especially soil samples and meeting the targets of the validation criteria. It is further aspired that the novel approach outperforms the established EOK during method comparison.

2 Materials and methods

2.1 Test sample set

A test sample set was used to evaluate the newly developed method by and compare it to the old one by measuring the CaOx content. The samples were collected in Kenya between the 17th and 18th of October 2022 in the scope of another study conducted by Rowley et al. (In prep). The sample site is located Samburu County, Kenya (Fig. 3). It is a dry and arid region with old plintho-, lepto-, and ferrasols that were formed on basalt flows or mixed metamorphic parent material. Samples were collected at three tree species: *Ficus Glumosa* (n = 5), *Ficus natalensis* (n = 3), and *Ficus sycomorus* (n = 5). Those three species have agroforestry potential by providing shade for crops and fodder for livestock, improving soil fertility and stabilising soil (Barnosky et al., 2004; Kassa et al., 2015; Sebuliba et al., 2022). Five different organic matter types, namely leaf, litter, bark, branch, and root, from each individual were sampled. That gives 65 plant samples in total. In addition, soil samples around each individual were collected as well. A transect of soil samples (0-20 cm depth) was collected with an auger adjacent (as close to the tree as possible), 1, 2, 3 m, and a control distance away from the tree (20 m). Besides the transect samples, one profile was sampled next to an individual of each species, sampling a profile adjacent and a control distance away from the tree (sampling at 0-2, 2-4, 4-6, 6-10, 10->25 cm depth). Adding the 95 soil samples to the 65 plant samples results in 160 samples for the sample set. Additional information about field work can be found in appendix A in table 15.

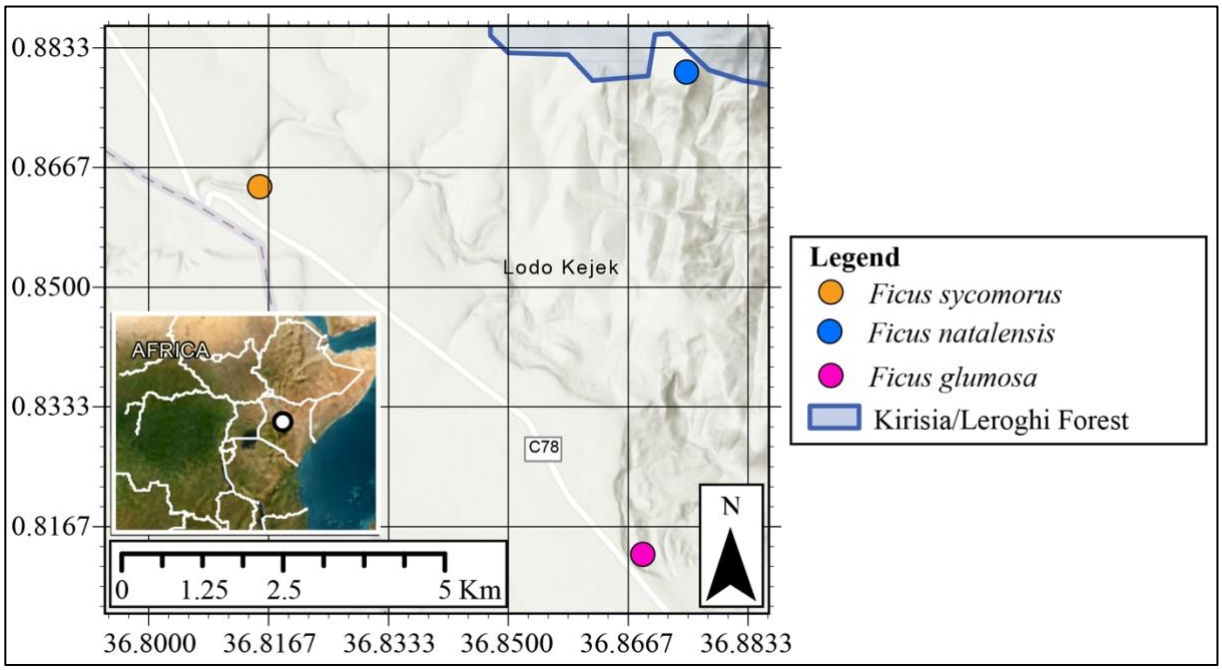

Fig. 3: Map of the study region and sampling sites. This map was constructed using basemap material (Esri, 2024).

2.2 Enzymatic oxalate analysis

Enzymatic oxalate analysis was conducted using a commercial EOK (Sigma-Aldrich, MAK 179 by Merck). Spiked quartz sand samples were analysed with the extraction procedure proposed by Certini et al. (2000). Specifically, 2 g of quartz sand was weighed out into 15 mL falcon tubes and spiked with $H_2C_2O_4$ (purified grade 99.999 % trace metals basis, Merck) at three different concentrations, 10.74 mg, 5.37 mg, and 3.16 mg. For extraction, 5 mL of 1 M hydrochloric acid (HCl) was added to each tube. Falcon tubes were shaken for 16 hours on the orbital shaker at 150 rounds per minute (rpm) and centrifuged for five minutes at 1100 g. 1 mL of supernatant was diluted with 4 mL of Milli-Q H_2O in a new 15 mL falcon tube and vortexed. With a 2 M sodium hydroxide (NaOH) solution pH values of the diluted extracts were neutralised. Additionally, a version that was diluted 1:20 with Milli-Q H_2O was prepared. Samples and standards were stored in the fridge at 3 °C. In addition to the standards provided by the kit, $H_2C_2O_4$ was diluted with Milli-Q H_2O to prepare two sets of own standards. The first set being concentrated at 0 mg/L, 10 mg/L 35 mg/L, 70 mg/L and 140 mg/L and the second one being 0 mg/L, 10 mg/L, 20 mg/L, 50 mg/L, 100 mg/L, 200 mg/L and 500 mg/L. For both standards also a 1:20 diluted version was also prepared. CaOx was quantified in a 96 well plate, following the instructions provided by the kit. Detailed amounts of each component added to the well plate are listed in table 1.

Tab. 1: Exact amounts of components added to the well plate for oxalate quantification with EOK

Sample/standard	Sample (µL)	Oxalate converter (µL)	Oxalate assay buffer (µL)	Master reaction mix (µL)
Provided standard	0, 2, 4, 6, 8, 10	2	50, 48, 46, 44, 42, 40	50
Own standard I	2.5	2	47.5	50
Own standard I	5	2	45	50
Own standard I	50	2	0	50
Own standard II	50	2	0	50
Spiked sand I	2.5	2	47.5	50
Spiked sand I	5	2	45	50
Spiked sand II	50	2	0	50

At first, the sample to be quantified, oxalate converter and oxalate assay buffer was added to the well plate. After incubating the well plate at 39 °C for an hour, the master reaction mix (consisting of 46 µL of oxalate development buffer, 2 µL oxalate enzyme mix, 2 µL oxalate probe) was added. The well plate was shaken for 5 min on the orbital shaker at 70 rpm to make sure the components mix well. The well plate was incubated again at 39 °C for an hour. Colour intensity was measured five times at 450 nm (MultiSkan Sky).

Based on the calibration curve obtained by the standards the oxalic acid concentration in mg/L of each spectrometer reading can be calculated and concerted into oxalic acid concentration mg/kg (Eq. 4). With equation 5, the previous result can be converted into the CaOx concentration.

$$H_2C_2O_4\ \left[\frac{mg}{kg}\right] = \frac{\frac{absorbance\ -\ intercept}{slope} * extraction\ volume\ [mL] * dilution\ factor\ [-]}{sample\ weight\ [g]}$$

Eq. 4: Conversion of spectrometer reading (absorbance) into $H_2C_2O_4$ (mg/kg)

$$CaOx\ \left[\frac{mg}{kg}\right] = H_2C_2O_4\ \left[\frac{mg}{L}\right] * \frac{observed\ CaOx's\ molar\ mass\ (142.11)\ \left[\frac{g}{mol}\right]}{observed\ H_2C_2O_4\ molar\ mass\ (90.03)\ \left[\frac{g}{mol}\right]}$$

Eq. 5: Conversion of $H_2C_2O_4$ (mg/kg) into CaOx (mg/kg)

Plant samples of the test sample set were already analysed with an EOK (Biotech Trinity) by Rowley et al. (In Prep.) in May 2023 at the University of California, Davis. CaOx was extracted with HCl (Certini et al., 2000) using methods outlined in (Rowley et al., 2017). These results will be included in this study as well.

2.3 High-performance liquid chromatography setup and analysis

In the following section the procedure of the final method is described that was developed and validated in this thesis. A detailed method development description and justifications for every parameter setting for sample preparation and quantification with HPLC can be found in section 3.

0.1 g of plant and 1.0 g of soil samples were balanced out in a 15 mL falcon tube. 5 mL of 10 M H_3PO_4 were added, and the tube was vortexed for 10 s. After shaking it for 16 hours (overnight) on the horizontal shaker at 150 rpm the tube was centrifuged at 1100 g for 5 min. The supernatant (about 4 – 4.5 mL) was filtered in a 6 mL glass column into another 15 mL falcon tube. Glass columns were prepared with a filter, sand (about 1 cm height) and some glass wool. Remaining solid sample material with the

remaining H_3PO_4, namely the cake, was vortexed for 10 s and 3 mL of 15 M H_3PO_4 was added to the tube. After vortexing the tube for 10 s, shaking it with the same settings on the horizontal filter for 30 min and centrifuging it with the same program, the supernatant was transferred with the same pipette and filtered with the same filter in the corresponding tube. The procedure was repeated once more for 2 mL of 15 M H_3PO_4, the third and last extraction step. Once filtered, the tubes with the collected extractants of the different steps were vortexed for 10 s. 1 mL of the extracts were transferred into a new tube, mixed with 4 mL of Milli-Q-H_2O for a 1:5 dilution and vortexed again for 10 s. For HPLC analysis 1 mL of the diluted extracts were transferred into an amber HPLC vial. The samples were ready for HPLC analysis and stored in the fridge at about 3 °C. Standards were prepared with oxalic acid (purified grade 99.999 % trace metals basis, Merck) and 2.5 M H_3PO_4 (phosphoric acid, 85+%, for HPLC by thermo scientific, diluted with Milli-Q-H_2O) at the following concentrations: 0 (blank H_3PO_4 sample), 0.5, 2, 5, 10, 20, 40, 80, 160 and 320 mg/L. To account for a potential intra-method shift the standards are analysed before and after the samples. Typically, about 20 samples were analysed in one extraction and subsequent HPLC sequence. Samples were analysed with the 1290 Infinity II HPLC system (Agilent) with the settings presented in table 1 and the program described in table 2. Solvent A had to be filtered prior to HPLC analysis with a Whatman glass fibre filter.

Tab. 2: Final HPLC method parameter settings

Parameter	**Setting**
Solvent A	400 mM H_3PO_4 (phosphoric acid, 85+%, for HPLC by thermo scientific)
Solvent B	acetonitrile (ACN, supragradient HPLC grade, Scharlau) and Milli-Q-water (1:1 diluted)
Flow rate	0.4 mL/min
Column type	2.1 x 150 mm Poroshell 120 SB-C_{18} (Agilent)
Number of columns	2 (identical)
Column temperature	8 °C
Injection volume	5 µL (standards and plant samples) 10 µL (soil samples)
Detection wavelength	210 nm

Tab. 3: HPLC method program for standards (without * after 10 min) and plant and soil samples (with * after 10 min)

Time (min)	Eluent A (%)	Eluent B (%)
0.00	99.90	0.10
10.00	99.90	0.10
15.00 / 11.00*	5.00 / 30.00*	95.00 / 70.00*
30.00 /19.00*	5.00 / 30.00*	95.00 / 70.00*
35.00 / 20.00*	99.90	0.10
60.00 / 35.00*	99.90	0.10
Post time: 5 min		

The expected chromatograms are displayed in figure 4 for a palnt sample (A) and a soil sample (B). A peak corresponding to oxalic acid occurred at 8.9 min. However, in the case of the soil sample, the entire double peak is used for further analysis.

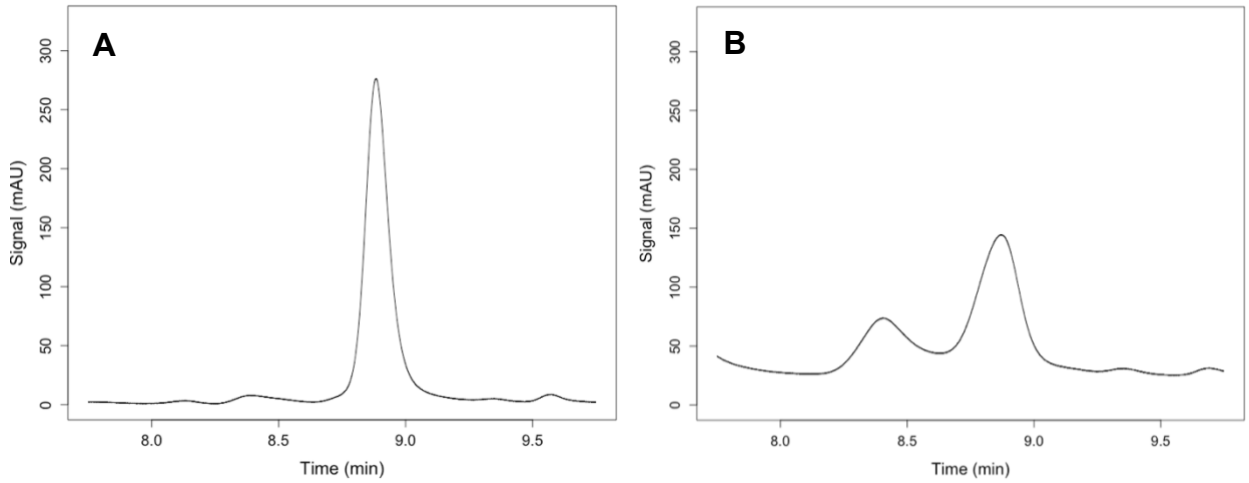

Fig. 4: Resulting chromatogram of an exemplary plant sample with a peak at 8.9 min (A) and the expected peak of a soil sample (B)

Based on the peak corresponding to oxalic acid, the peak area could be integrated with Agilent Lab Advisor Software (OpenLAB CDS ChemStation Edition, Agilent Technologies). The oxalic acid concentration (mg/kg) can be determined with equation 6 for plant samples and 7 for soil samples. Converting the result into CaOx (mg/kg) can be done with equation 5.

$$H_2C_2O_4\ \left[\frac{mg}{kg}\right] = \frac{\frac{peak\ area\ -\ intercept}{slope} * extraction\ volume\ [mL] * dilution\ factor\ [-]}{sample\ weight\ [g]}$$

Eq. 6: Conversion of the integrated peak area into $H_2C_2O_4$ (mg/kg) for plant samples

$$H_2C_2O_4\ \left[\frac{mg}{kg}\right] = \frac{\frac{1}{2} * \frac{peak\ area\ -\ intercept}{slope} * extraction\ volume\ [mL] * dilution\ factor\ [-]}{sample\ weight\ [g]}$$

Eq. 7: Conversion of the integrated peak area into $H_2C_2O_4$ (mg/kg) for soil samples

3 Method development

3.1 Extraction and sample preparation

The extraction process used in combination with the EOK served as a starting point for the new extraction method (Certini et al., 2000; Rowley et al., 2017). During the development process, different parameters were adapted by finding the best choice out of a set of different options. Fig. 5 presents the adapted parameters, their corresponding options and the best choice that was selected. It was focused on the acid and its molarity used for extraction, the number of extraction steps, pH adjustment of the extracts and how they should be diluted. The filtration which was also a parameter that was optimised, is not included in the flow chart because it does not affect the actual extraction efficiency, only the applicability of the method.

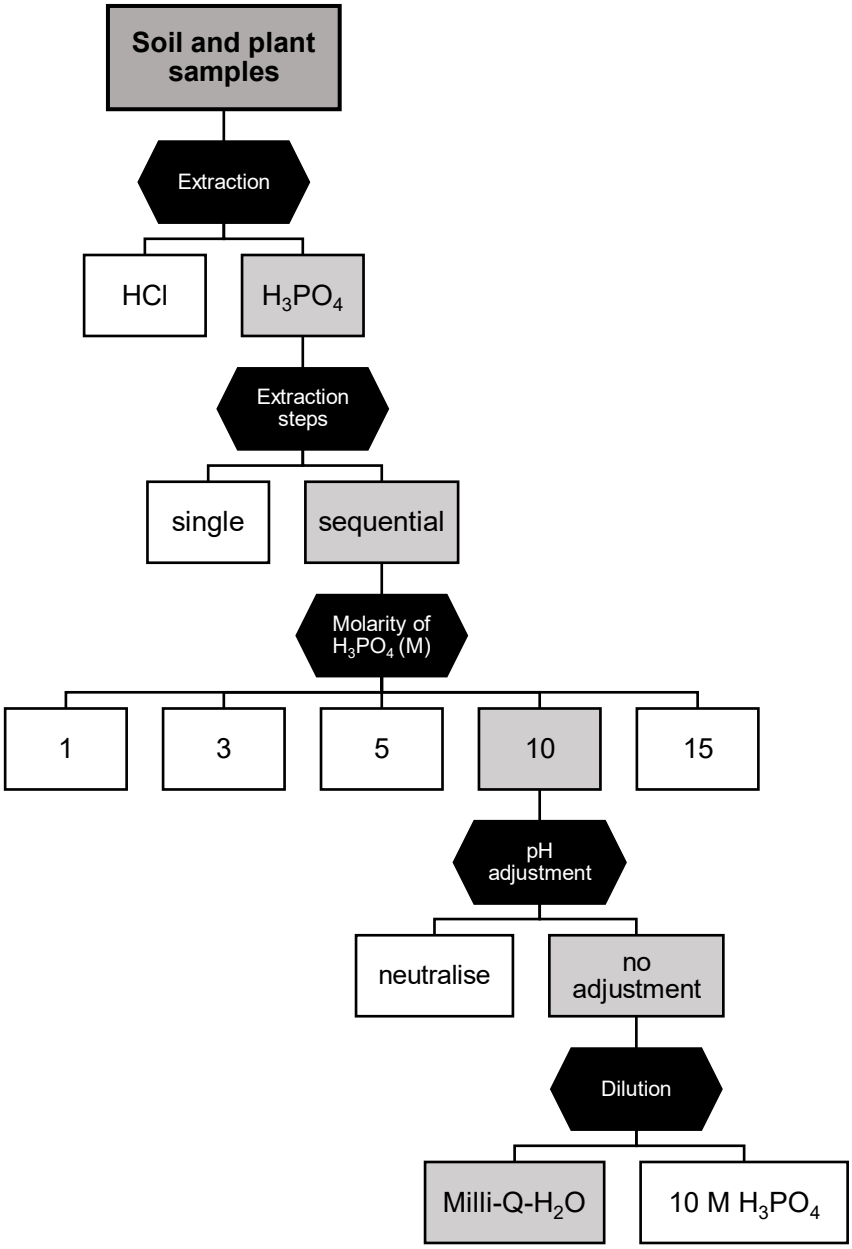

Fig. 5: Decision tree of the optimised extraction and sample preparation procedure (source: own graphic)

Different criteria were used to validate which option is the best. Naturally, the main criterion was the extraction efficiency. It was determined by the peak area of the chromatogram of the target compound measured with the HPLC method. Thus, it is important to highlight that the HPLC method was designed before and during the development process of the extraction method, and the descriptions are not chronological. An accurate validation of the different options would not have been possible otherwise. It was further focused on peak shape. A Gaussian peak is an indication of a well-behaved instrument without any column packing issues or interferences by other compounds (Wahab & Armstrong, 2017). If no or only a very small difference in extraction efficiency was measured, the least time-costly option was chosen.

Selection of acid and molarity

Extracting with 1 M HCl proposed by Certini et al. (2000) and injecting HCl into the HPLC system would lead to corrosion, which could damage metal parts and seals. Since it was already established that the main fraction of the HPLC eluents is H_3PO_4 (see chapter 3.2), it was a reasonable option to use H_3PO_4 for extraction as well. Due to the low concentration of CaOx and complex matrix, soil samples could not be detected with the detection method by HPLC at this stage of the development process. Therefore, the focus was set only on organic matter samples. To do so, a litter sample was extracted with 1 M HCl, 1M, 3 M, and 5 M H_3PO_4 with the established procedure and measured by HPLC. Since oxalic acid is a photoactive acid, the tubes were covered during extraction to reduce the production of free radicals (Tasdelen et al., 2008). Three samples for each acid and molarity were analysed. The peak shapes in the resulting chromatograms all followed a bell shape, confirming the good data quality. Therefore, the CaOx concentration based on the integrated peak was computed and compared (Fig. 6). The means of the extracted CaOx concentrations of the 1 M HCl, 3 M, and 5 M H_3PO_4 extraction lie in a comparable range. Compared to the 3 M H_3PO_4, the mean is slightly larger and the standard deviation is smaller for the 5 M H_3PO_4 extraction. Therefore, the 5 M H_3PO_4 extraction was considered to be the best option.

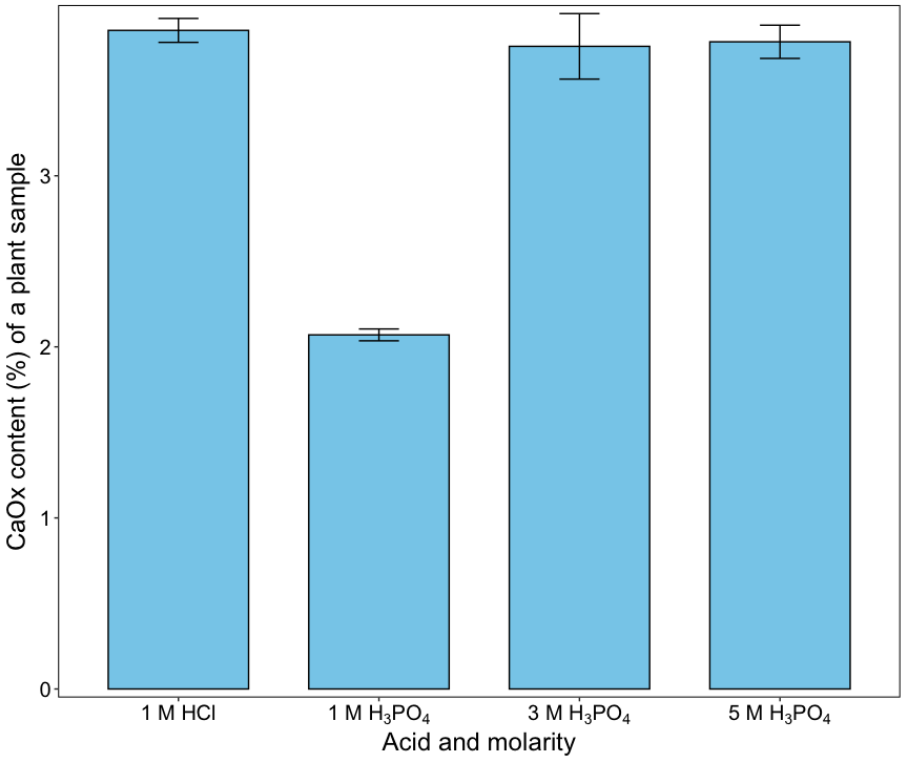

Fig. 6: Yielded CaOx content (%) extracted with 1 M HCl and 1, 3 and 5 M H_3PO_4 of a litter sample

The small difference in the extraction efficiency between the 3 M and 5 M H_3PO_4 treatment shows that an increase in the molarity is no longer very effective as it exceeds 3 M. In the case of the plant samples with a generally high CaOx concentration compared with soils, a 5 M H_3PO_4 extraction would thus be sufficient. To make sure that the method is also suitable for soil samples where CaOx concentrations are smaller, a 10 M H_3PO_4 extraction was tested as well and compared to the 5 M H_3PO_4 treatment. Naturally, this could only be done after the method was further developed for soil samples. A random soil sample was extracted and measured with HPLC for this purpose. Both peak shapes followed a bell curve, but the extraction efficiency was about 15 % larger for the 10 M H_3PO_4 treatment (Fig. 7), indicating that an increase in molarity was still very beneficial for soil samples. By comparing a spiked soil sample at a molarity of 5 M and 10 M, as well, a spike recovery of about 65 % for the 5 M H_3PO_4 extraction and a recovery of about 85 % for the 10 M H_3PO_4 treatment was found, confirming the previous finding. Therefore, the 10 M H_3PO_4 option was selected to build on for further method development. A higher molarity of the acid leads to a higher viscosity, which can make further sample preparation, such as filtration more complex. Therefore, it was decided not to increase the molarity of H_3PO_4 and rather implement several extraction steps, i.e., a sequential extraction, to improve the extraction efficiency even more.

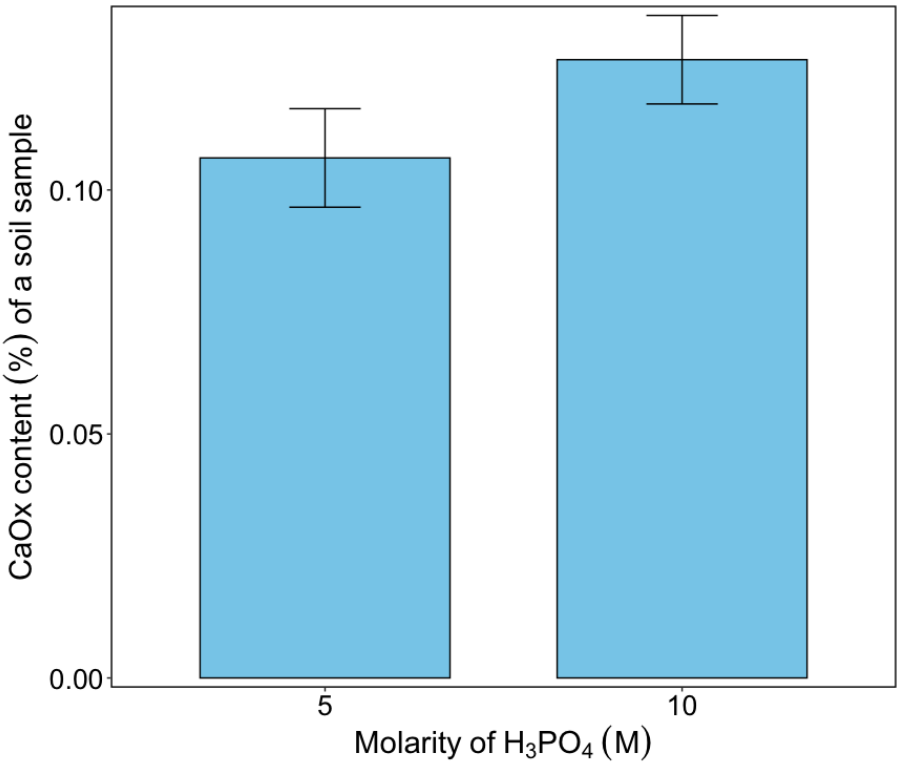

Fig. 7: Yielded CaOx content (%) extracted with 5 M and 10 M H_3PO_4 of a soil sample

Single vs. sequential extraction

In the previous step, an extraction with 5 mL of 10 M H_3PO_4 was already established. This step served as the first step of the sequential extraction. Two additional steps were added to the procedure to increase the extraction efficiency even more. In both steps 15 M H_3PO_4 were used, 3 mL for the second and 2 mL for the third step. Combining these three steps resulted in a 12.5 M H_3PO_4 solution.

The extraction efficiency of every step was tested with a randomly chosen plant and soil sample. To do so, the samples of both sample types were weighed out twelve times each, as previously stated. The first nine samples were extracted with one of the extraction steps separately in triplicate, while the entire sequential extraction was performed on the fourth sample, also in triplicate. The CaOx content of each sample was quantified with the HPLC method. By comparing the obtained CaOx contents of every single step to that of the combined sample, the extraction efficiency of the separate steps could be broadly assessed (Fig. 8). During the first extraction step, about 75 % of the plant and 65 % of the soil could already be extracted. After that, only a small increase in extraction efficiency can be observed. It is noticeable that for the soil samples extraction steps 2 and 3 contribute more to the extraction than these steps in the plant sample. In total, slightly more CaOx is extracted in the case of the plant sample. However, both values range around 90 %, suggesting a good extraction efficiency for both sample types. As the increase in extraction efficiency is not in

proportion to the additional time required by introducing further extraction steps, the method was limited to these three steps.

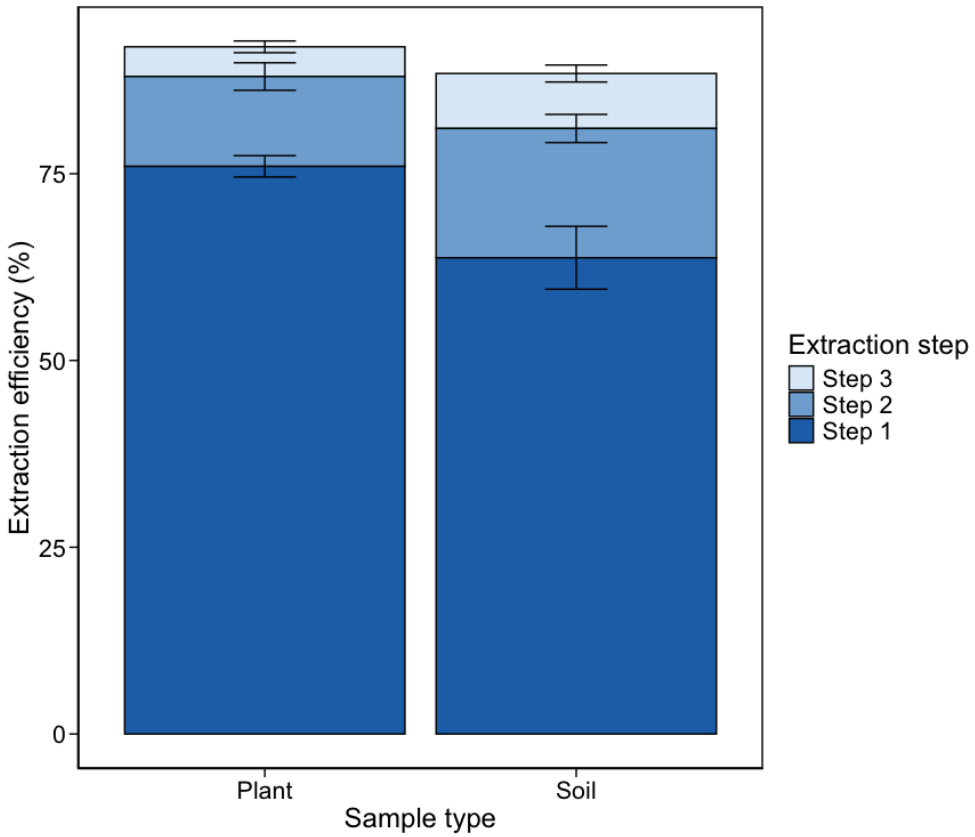

Fig. 8: Extraction efficiency of a three-step sequential extraction of a plant and soil sample

Adjustment of pH

So far, only neutralised extracts, i.e., samples with a pH ranging between 5 and 7, could be analysed by the EOK. Since the pH value of the extracts was around 1, every sample had to be neutralised by adding a certain amount of 2 M NaOH. Estimating the right amount of NaOH was difficult. Thus, the procedure was very time-consuming and adding more substances to the sample could potentially affect the results of the measurement. Therefore, it was tested if skipping this step was possible while still obtaining the same results, such as peak area and shape in the chromatogram.

A randomly chosen organic matter sample was extracted, and two HPLC samples were prepared, one neutralised and the other one without any adjustment of the pH. The neutralised sample resulted in a slight peak broadening and peak distortion compared to the untreated sample. Therefore, pH adjustment could be excluded, which makes the procedure more time-efficient.

Dilution

The last step of the sample preparation process that influences the actual measurement was the dilution of the extracts. It is necessary to reduce potential interference with other compounds in the sample, such as minerals or pigments. By diluting the samples, this matrix effect will be reduced to a point at which the measurement will not be skewed. Diluting the samples further avoids saturation of the detector during the analysis. The first dilution option that was tested was the 1:5 dilution with Milli-Q H_2O suggested by the EOK. Since the eluent of the HPLC analysis will consist mainly of H_3PO_4 (see chapter 3.2), it was also tested whether the acidification of the extract is beneficial in terms of peak area or shape. To do so, the Milli-Q H_2O was replaced by 10 M H_3PO_4 for the dilution of a random plant and soil sample. However, the chromatograms of the plant (Fig. 9, A) and soil sample (Fig. 9, B) reveal that acidification is not beneficial. Diluting the extracts of the plant sample with Milli-Q H_2O results in a desired bell-shaped peak. However, after acidification, the peak widens and does not follow a bell shape anymore. In case of the soil sample, the two distinct peaks resulting from a dilution with Milli-Q H_2O are merged after acidification to one weirdly shaped peak, which is not usable for oxalate quantification. Consequently, the 1:5 dilution with Milli-Q H_2O was chosen.

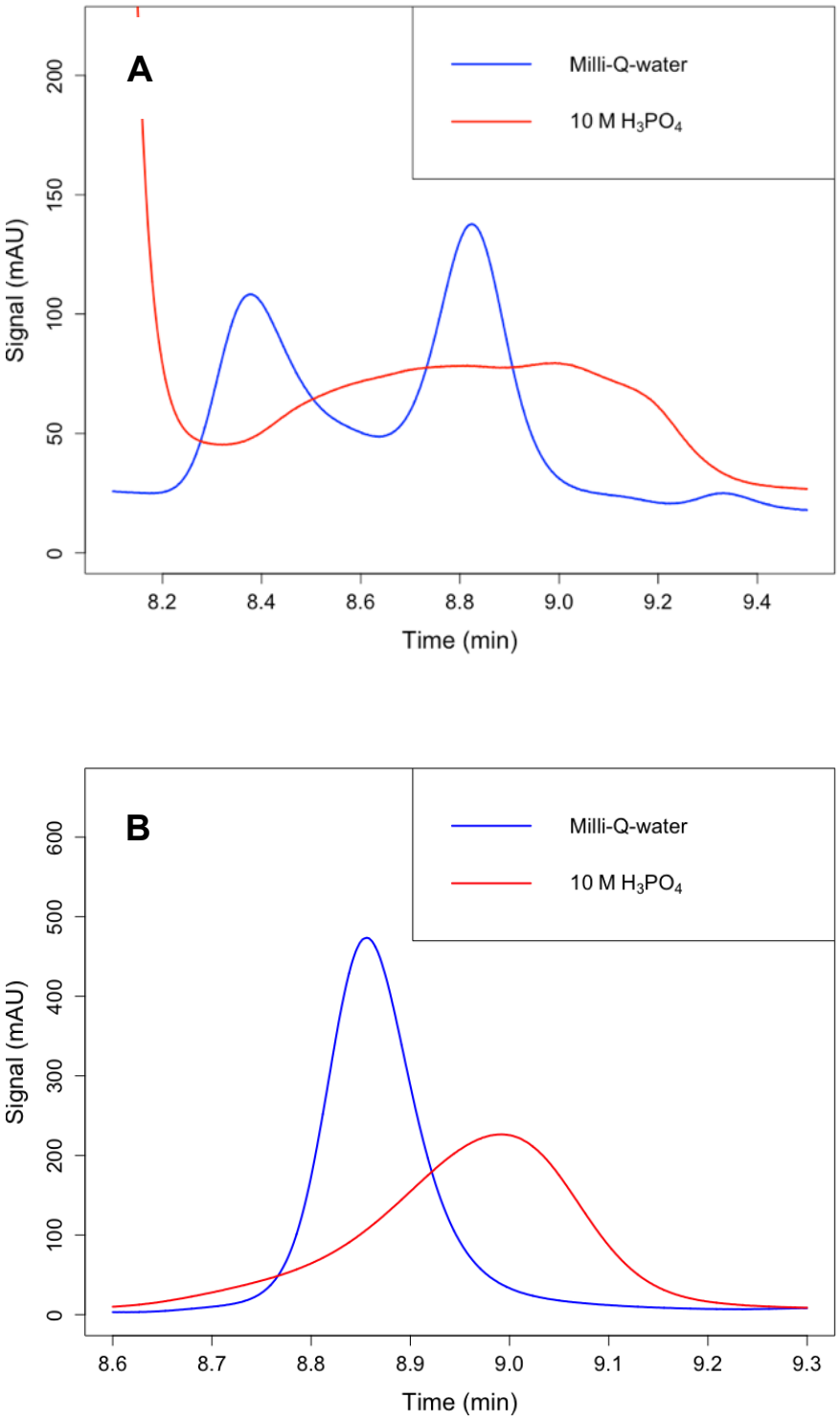

Fig. 9: Chromatogram of a plant sample extract diluted with Milli-Q H_2O (A) and with 10 M H_3PO_4 (B)

Filtration

Filtering the extracts is indispensable to prevent the HPLC system from damages through clogging. This step was not added as an adjusting parameter in the decision tree because filtering the samples does not affect the measurements' results. However, an optimised filtration procedure saves time and energy allowing a higher rate of sample preparation. Thus, the optimization process focused on making the filtration part more time-efficient.

Increasing the molarity of H_3PO_4 and implementing several extraction steps led not only to an improvement in the extraction efficiency but also to dissolving more organics and particles, especially for the plant samples. As a result, filtering the extracts became slower, and several adjustments had to be made. In a first step, 6 mL instead of 3 mL glass columns were used (Fig. 10, A). Those columns have a larger diameter and allow thus faster filtration. Since the filter was still almost clogged, glass wool (Fig. 10, B) and quartz sand (Fig. 10, C) had to be added on top of the filter to increase the surface area. Combined with a vacuum pump, the samples could be filtered within 12 to 24 hours. Consequently, this setup was chosen for the following sample preparation.

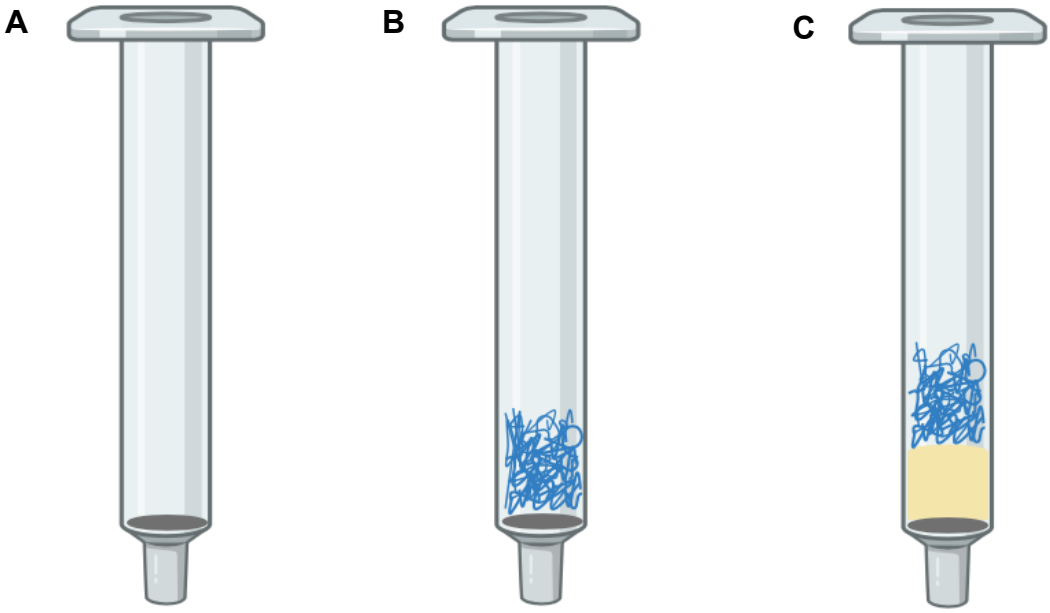

Fig. 10: First filtration setup with filter (grey) only (A), second setup with filter and glass wool (blue; B) and improved third and final filtration setup with a filter, sand and glass wool (yellow; C). Created in https://BioRender.com (06.03.2025)

3.2 Quantification with high-performance liquid chromatography

For the development of the HPLC method the same trial and error procedure applied as for to the extraction method. Different parameters were optimised by finding the best choice out of a set of options (Fig. 11).

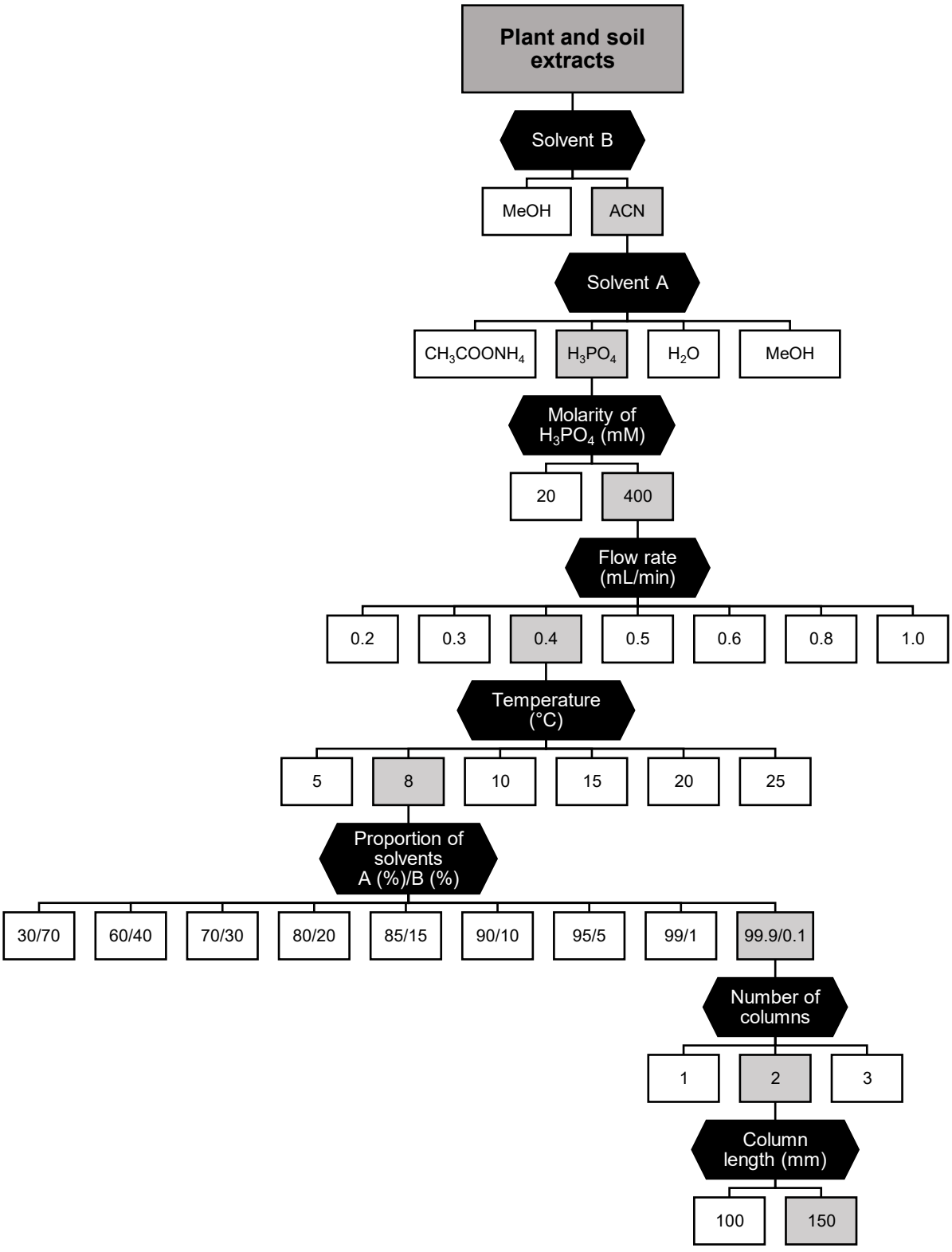

Fig. 11: Decision tree of the developed HPLC method (source: own graphic)

It was focused on the following parameters: Solvent A and B and their proportion, flow rate, temperature of the column, column length, and number of columns. Further, the injection volume, detection wavelength and the program were optimised as well. They are not included in the decision tree because they do not influence the quantification method directly. In the case of the injection volume and the program, they depend on the kind of sample (standards, plant, or soil sample) that is analysed and are therefore adapted frequently.

To assess the quality of the different options and decide which one should be selected, it was again mainly focused on the chromatogram. Firstly, the target compound had to be separated from other compounds in the sample. This was achieved by increasing the retention time of the corresponding peak. In other words, the chromatogram was stretched out. Therefore, parameter settings that shifted the retention time of the oxalic acid peak backwards were chosen. Along the way, the shape and width of the peak are also focused on. Besides the chromatogram, other factors, such as applicability, expenses and the level of throughput also played an important role. Sometimes, only tiny changes and improvements can be observed by switching from one option to another. In those cases, the least expensive, best applicable or the most efficient in terms of throughput was chosen.

Finding a starting point

Initially, a starting point had to be found to quantify oxalate. Based on these settings the method could be optimised by further adjustments. To do so, literature research on previous HPLC methods quantifying oxalate was conducted. The focus was on the following parameters including column type, eluents and eluent composition, flow rate, temperature, gradient, detector and detection wavelength, and injection volume. Six previous methods quantifying CaOx were found and their values for each of the previously named parameters were collected (Tab. 4). To select a method to start with the proposed columns were compared to the inventory of the columns in the lab because columns for HPLC analysis are rather costly. Luckily, a similar C_{18} column to the one available in the laboratory was used by Shen et al. (2021). Therefore, the parameters of this method were selected as a starting point.

The eluent and eluent composition, flow rate, temperature, and detection wavelength were set as described. The method was tested with a 70 mg/L oxalic acid standard already used with the EOK. Since there was no information about the injection volume it was set to 3 µL. A retention time of about 13 min was suggested. Nonetheless, after about 15 min the run was stopped because no peak could be observed. One possible explanation for the absence of a peak could be a concentration of the standard. The injection volume was thus increased to 20 µL and a second run was started. Despite a

larger concentration of the target compound, no oxalic acid could be detected with the selected settings after about 15 min. After having a look at the paper by Shen et al., (2021) again it was found that the sample was derivatised with o-phenylenediamine (OPD). This detail was overlooked by reading the paper and another starting point had to be found.

As a second attempt a method developed for benzene polycarboxylic acid (BPCA) was tested. The method was also created in the lab of the Department of Geography at the University of Zurich (Wiedemeier et al., 2016). Only the solvent composition, which was 99.5 % 20 mM H_3PO_4 (solvent A) and 0.5 % acetonitrile (ACN; solvent B) of the BPCA method was used. The other parameters, previously described, remained unchanged. With these settings, a peak at 1.03 min could be observed in the chromatogram. With that a starting point was found from which the method could be further optimised.

Selection of solvent and their proportion

Based on the starting point given by the BPCA method it could be continued with selecting solvents and optimising their proportion. A list with the detailed changes of every parameter during the entire HPLC method development process can be found in appendix B, table 16.

In a first step, methanol (MeOH) instead of 20 mM H_3PO_4 was tested again, in this case for solvent A. Solvent B remained unchanged. During the first run a 70 mg/L oxalic acid standard was measured with 90 % MeOH and 10 % ACN. In steps of 10 %, the amount of MeOH was reduced to 30 %, and the amount of ACN was increased during each run. The retention time was shifted from 0.74 min to 0.81 min. Based on these results, it can be said that in combination with ACN, a decrease of MeOH leads to a larger retention time. However, comparing these retention times to the very first one of 1.03 min achieved by using 20 mM H_3PO_4 instead of MeOH, it was reasonable to assume that H_3PO_4 might be more suited for the method. Therefore, MeOH was replaced by 20 mM H_3PO_4 for solvent A. Solvent B remained again unchanged. By testing 30 %, 20 %, 10 % and 0.5 % of 20 mM H_3PO_4 a retention time between 2.27 min and 2.36 min was determined. Interestingly in contrast to MeOH, a decrease of ACN was favorable for increasing the retention time. Based on these findings it was decided to use H_3PO_4 for solvent A and ACN for solvent B. To assess if the molarity of the H_3PO_4 influences the retention time a 400 mM H_3PO_4 was tested at different concentrations. The increase of molarity shifted the retention time backwards. It could be confirmed that more H_3PO_4 led to an increase in retention time. Therefore, 99.9 % of 400 mM H_3PO_4 and 0.1 % of ACN was chosen as a final solvent composition.

Tab. 4: Parameter settings for quantification of oxalate by HPLC of other studies

Study	Column	Solvent	Flow rate	Temperature	Gradient	Detector / detection wavelength	Injection volume
Castellari et al., 2000	Aminex HPX-87H column (300 × 7.8 mm) protected with a pre-column (30 × 4.6 mm)	0.003-0.05 N sulphuric acid with 6 % acetonitrile (v/v)	0.5 mL/min	45 °C (both columns)	isocratic	210 nm	20 µL
Hunt et al., 2004	Ion-300 organic acid analysis column	0.005 N sulphuric acid	0.5 mL/min	67 °C	isocratic	210 nm	80 µL
Hönow & Hesse, 2002	Anion exchange column	2 g EDTA/L distilled water was adjusted to pH 5.0 (by adding 15 ml 0.3% NaOH)	-	-	-	amperometric	-
Savage et al., 2000	Aminex Ion exclusion HPX-87H analytical column (300 × 7.8 mm) attached to an Aminex cation H+ guard column	0.0125 M sulphuric acid	0.5 mL/min	25 °C (analytical column)	isocratic	210 nm	5 µL
Savage et al., 2004	Ion exclusion column (300 × 7.8 mm) attached to a cation H+ guard column	aqueous solution of 25 mM sulphuric acid	0.6 mL/min	25 °C (analytical column)	isocratic	210 nm	20 µL
Shen et al., 2021	Phenomenex Luna C_{18} column (250 × 4.6 mm, particle size 5 µm)	15 % methanol in water containing 0.17 M ammonium acetate	1 mL/min	25 °C	isocratic	314 nm	-

Selection of flow rate

Another parameter that affects the retention time is the flow rate. A smaller flow rate leads to an increase in retention time because the sample extract passes the column more slowly. However, it results in a widening and distortion of the peak shape, such as fronting or tailing. Therefore, a balance must be made between a desired increase of retention time and an undesired broadening and distortion of peak shape.

Optimal flow rate was determined by using 30 % of 20 mM H_3PO_4 (A) and 70 % of ACN (B). An initial flow rate of 1.0 mL/min resulted in a retention time of 0.81 min. Another six different flow rates were tested: 0.8, 0.6, 0.5, 0.4, 0.3 and 0.2 mL/min and their retention times, their peak shapes and widths compared (Tab. 5). As expected, a decreasing flow rate resulted in a larger retention time but also in a broadening of the peak. Down to a flow rate of 0.4 mL/min the peak was shaped as a symmetric bell shape. This shape was not observed anymore for the flow rates of 0.3 and 0.2 mL/min. Therefore, it was decided that the optimal flow rate for this method is 0.4 mL/min. It is small enough to maximise the retention time and large enough to result in a symmetric bell-shaped peak.

Tab. 5: Retention times, width and peak distortions at different flow rates

Flow rate (mL/min)	Retention time (min)	Width (s)	Peak distortion
1.0	0.81	19	Fronting
0.8	1.0	20	Fronting
0.6	1.32	23	Fronting
0.5	1.85	27	Fronting
0.4	2.30	37	Some tailing
0.3	3.07	49	Tailing
0.2	4.61	79	Tailing

Selection of column temperature

Column temperature also has an impact on retention time. Thus, it was tested whether it should be increased or decreased. This was done with 90 % of 400 mM H_3PO_4 (A) and 10 % of pure ACN (B) at an isocratic flow and a flow rate of 0.4 mL/min. Starting from a temperature of 25 °C, the column was cooled down gradually in steps of 5 °C down to 10 °C. At this stage, the peak appeared at 2.585 min. In the chromatogram at 20 °C, the retention time of the oxalic acid peak was slightly shifted backwards (by 0.012 min). Decreasing the temperature to 15 and 10 °C caused a larger shift backwards in time. This observation led to the conclusion that a cooler column temperature results in a shift backwards in time of the peak, while the peak

shape still follows a bell shape. However, a cooler temperature also increases the chances of condensation around the column in the HPLC apparatus. The resulting condensation water does not necessarily damage the device. Nonetheless, the sensor cannot distinguish between a leak and condensation water. In both cases, the sequence will be stopped automatically. To avoid such unnecessary interruptions, the temperature should be selected as high as possible. Therefore, only the temperatures 8 °C and 5 °C were tested. The retention time shift was with 2.645 min 0.01 min larger at 5 °C than at 8 °C. Since the lower risks of condensation at a higher temperature outweigh the negligible small difference in retention time, it was decided against 5 °C. As a result, the column was set to a temperature of 8 °C for future tests.

Selection of column number and column length

So far, one C_{18} column has been used during method development process. The bell shaped, symmetric peak of the oxalic acid standards and plant samples chromatograms indicated that the properties of the stationary phase was suited for quantifying CaOx in combination with the other parameters of the method. The column characteristics thus should be retained in terms of chemistry. However, the resulting chromatogram of the soil samples was still not entirely satisfying with an unknown peak very close to the peak of the target compound. Ideally, these two peaks could be separated until the signal between them goes down to the baseline. In other words, the chromatogram should be stretched out. One option to do so is to change the number and length of the columns.

Hence, a second identical column was added to the system in a first step. Since the sample extracts had to pass twice the way through the columns, the retention time doubles, and the chromatogram is stretched out. The retention time of the oxalic acid standard was shifted from 3.03 min to 6.1 min. Nonetheless, the two peaks were still not separated, and further adjustment was needed. Using a longer column also leads to a stretching effect of the chromatogram. Luckily, two identical C_{18} columns with a length of 150 mm were available in the laboratory. In this second step, the retention time was shifted to 8.9 min, and the peak separation of the soil chromatogram was improved. The peak separation was not ideal yet, thus a third C_{18} column was installed. Despite three columns, the peaks were still not fully separated. It only led to a broadening of the peaks and an extension of the entire method. Further, the monetary aspect should be taken into consideration as well. The tiny improvements do not stand in any relationship with the costs. As a result, it was decided to stick with the two 150 mm C_{18} columns.

Injection volume

Introducing the right amount of extract into the HPLC system is essential for an accurate quantification of the target compound. A too large injection volume would lead to an oversaturation of the stationary phase, which results in poorly shaped peaks. If the injection volume is too small, the detection signal might be too weak for reliable results. There might be further issues with repeatability due to a larger influence of small variations. Hence, the optimal injection volume had to be determined. During the development process, it became quickly apparent that the initial injection volume of 20 µL was too large for plant samples, and an oversaturation could be observed. Consequently, it was reduced to 10 µL, which was still led to column overload, and 5 µL were injected. Based on the peak shape, this was the right choice. Since the standards are in a similar range of oxalate concentration, the same injection volume was selected. Due to their much lower oxalate concentration, the amount of soil sample extract was doubled to quantify it precisely. Ultimately, it was decided to inject 5 µL of the standards and plant samples and 10 µL of the soil samples.

Selection of detection wavelength

At first, oxalic acid was detected at a wavelength of 216 nm because it was the one proposed by the BPCA method that served as a starting point (Wiedemeier et al., 2016). However, numerous studies suggest using a detection wavelength of 210 nm (Tab. 4). Therefore, the wavelength was set to 210 nm. To make sure that the peak of oxalic acid can be identified in more complex plant and soil samples the wavelengths 200, 230 and 280 nm were also used. The proportion of their heights of the signals acts as a fingerprint of the target compound, and detection is clearer than to focus solely on the retention time.

Program

Quantifying CaOx at around 8.9 min would suggest that the run can be stopped shortly after this time and the next sample can be analysed. However, the program does not end when the target compound is quantified. With every measurement some residue of the sample can accumulate in the HPLC system and may interfere with subsequent analysis, leading to wrong results. Furthermore, phosphoric acid is producing phosphate crystals, if not properly flushed through the system. Therefore, the column should be cleaned after every analysis by flushing it with an organic solvent, such as ACN or isopropanol, for several minutes. After cleaning and setting the solvent proportions back, the pressure and baseline of the signal is unstable due

to the change in solvent. That could lead to wrong peak areas, and thus, it should be waited a few minutes until a straight pressure curve and baseline indicate that the system is ready for the next measurement. To automate the method, i.e., when running a sequence, the cleaning and baseline stabilising step can be included in the program by changing the proportion of solvents (Tab. 6). Duration of each step has been determined by setting a time and checking the signal and pressure curve for larger changes. Since standards contaminate the system less than actual soil or plant samples, a shorter program has been developed for standards as well. This approach saves time, solvent and increases throughput.

Tab. 6: Final HPLC program with reasoning for plant and soil samples and standards (*)

Time (min)	Solvent A (%)	Solvent B (%)	Reasoning
0.00	99.90	0.10	Measuring CaOx
10.00	99.90	0.10	
15.00/11.00*	5.00/30.00*	95.00/70.00*	Cleaning column
30.00/19.00*	5.00/30.00*	95.00/70.00*	
35.00/20.00*	99.90	0.10	Stabilising baseline
60.00/35.00*	99.90	0.10	
Post time: 5.00 min			

4 Method validation

4.1 Validation criteria

Assessment and subsequent comparison of the EOK and HPLC method was conducted based on a set of validation criteria with an expected target (Tab. 7). The criteria linearity, limit of quantification, recovery and repeatability evaluate the methods from an analytical point of view (Raposo & Ibelli-Bianco, 2020), whereas the criteria sample stability, costs and applicability focus in on logistics.

Tab. 7: Validation criteria with their corresponding procedure and expected target

Criterion	Metric	Target
Linearity	R^2, slope, intercept and value of y at x maximum COV (coefficient of variation) model values of standard concentrations	$R^2 \geq 0.999$ Differences between standard curves as small as possible COV model ≤ 10 %
Limit of quantification (LOQ)	Lowest limit (standard concentration) at which the compound can be quantified. Upper limit is the higher end of the standard curve.	-
Spike recovery/ extraction efficiency	Extract and analyse a spiked blank (spike recovery) or an actual spiked sample (extraction efficiency) and assess the percentual recovery	80 % recovery
Repeatability	Assess difference in CaOx content between field replicates	EOK: 10 % difference (single step extraction) HPLC: 20 – 30 % difference (multi step extraction)
Sample stability	Assess percentual change in CaOx content of the same random sample measured several times over the time of validation	-
Costs	Assess costs for a sample run in duplicate.	-
Applicability and time expenses	Assess time for running the procedure once and state time-consuming steps	-

4.2 Enzymatic oxalate kit results

The EOK was mainly evaluated with the data obtained by the Sigma-Aldrich EOK. Since no actual samples of the sample set could be analysed in the framework of this thesis, the data obtained with the Biotech Trinity EOK of the study conducted by Rowley et al. (In prep) are included as well.

Linearity

To assess the linearity of the Sigma-Aldrich EOK slope (m), intercept (b), value of y at a maximum x value (x_{max}), also called endpoint in this thesis, and R^2 of the five standard curves are analysed (Tab. 8). By focusing on the first and last standard curve, based on the very small R^2 the curve cannot be considered linear. Thus, they are useless for further oxalate quantification. The other three standard curves in the middle consist of the same standard concentrations (1st standard) at different dilution factors and based on the R^2 the linearity can be regarded as good. However, the large variability (relative standard variation (RSD) = 59.90 %) of R^2 values across different calibration curves show that the method is highly unreliable and not robust to changes such as dilution factor. This finding is also supported by the large RSDs of slope, intercept and endpoint values.

Tab. 8: Evaluating parameters of different calibration curves obtained with the Sigma-Aldrich EOK

Date of measurement / standard curve	**m**	**b**	**y at x_{max}**	**R^2**
13.06.2024 / their standard	0.0223	0.1388	0.944	0.560
13.06.2024 / 1st standard, DF 20 afterwards	0.0022	-0.0009	0.281	0.998
13.06.2024 / 1st standard, DF 10 afterwards	0.0012	0.0242	0.322	0.965
20.06.2024 / 1st standard, DF 20, before	0.00022	0.00070	0.0287	0.997
20.06.2024 / 2nd standard, DF 20, afterwards	0.000018	0.1841	0.193	0.0254
Absolute mean	0.0052	0.0697	0.3537	0.709
Relative standard deviation (%)	185.16	122.99	98.56	59.90

The results of the COV model (Tab. 9) underscore these findings. Very large COV model values of the first standard curve and especially of the last one suggests a bad linear model fit as well. The three remaining standard curves indicate a better, mainly acceptable, model fit. Generally, model fit is worse at small concentrations compared to higher ones.
In summary, the linearity of the Sigma-Alderich EOK is highly unreliable and therefore cannot guarantee a proper oxalate quantification.

Tab. 9: COV model values at different concentrations obtained with the Sigma-Aldrich EOK

Date of measurement / standard curve	**Standard concentration (mg/L)** / **COV model (%)**					
13.06.2024 / their standard	180.06	360.06	540.18	720.24	900.30	
	207.8	-198.4	38.0	12.3	-65.3	
13.06.2024 / DF 20, afterwards	10	35	70	140		
	13.72	2.01	-6.43	1.41		
13.06.2024 / DF 10 afterwards	10	35	70	140		
	-34.94	44.91	8.07	-4.64		
20.06.2024 / DF 20 afterwards	10	35	70	140		
	-3.71	13.92	0.61	-0.99		
20.06.2024 / DF 20, before	10	20	50	100	200	500
	-2575.54	5020.30	1104.80	-2441.58	340.67	22.32

By looking at the standard curves of the other study (Rowely et al., In prep) the linearity of the Biotech Trinity EOK can also be assessed. The standard curve consisting of 0 mg/L, 10 mg/L, 50 mg/L, 100 mg/L and 200 mg/L were measured seven times. In table 10 the slope, intercept, value of y at x_{max} and the R^2 are displayed. Based on the R^2 the linearity is in six out of seven ≥ 0.999 which is great. The second standard curve measured on the 26th of May not only differs in the value of R^2 from the other standards, but also the other three values. This suggests that some external factor might have influenced the measurement, and the results should be viewed with some caution. Leaving this standard by the side, the values of R^2, of the slope and values of y at x_{max} show little difference and RSD, indicating a robust and reliable linearity of the method. However, the intercept values are variable compared to the other parameters, suggesting a better model fit for large concentrations compared to small concentrations. By looking at the COV model values (Tab. 11) this finding is confirmed. Generally, the difference between predicted

and actual value is very small and mainly lies in the acceptable range. However, the most deviating values are found at small concentrations. Again, the second standard run shows the largest differences throughout the entire set of standards.
In conclusion, the linearity of the Sigma-Aldrich EOK is not sufficient. It further seems to depend on dilution factors, where it was diluted and unknown external factors. That makes the method highly unreliable. The Biotech Trinity EOK shows a great linearity and a high method ruggedness.

Tab. 10: Evaluating parameters of different calibration curves obtained with the Biotech Trinity EOK

Date of measurement	**m**	**b**	**y at x_{max}**	**R^2**
24.05.2023	0.0119	-0.0964	2.29	0.999774
26.05.2023	0.00897	0.0953	1.89	0.996497
02.06.2023	0.01116	0.0522	2.29	0.999553
13.06.2023	0.01156	0.0832	2.40	0.999927
15.06.2023	0.01152	0.0899	2.40	0.999692
22.06.2023	0.01139	0.102	2.38	0.999727
30.06.2023	0.01140	0.0774	2.36	0.999801
Absolute mean	0.0111	0.0852	2.29	0.999282
Relative standard deviation (%)	8.79	19.67	7.93	0.12

Tab. 11: COV model values at different concentrations obtained with the Biotech Trinity EOK

Date of measurement	**Standard concentration (mg/L)**			
	10	**50**	**100**	**200**
24.05.2023	-12.85	1.43	1.35	-0.39
26.05.2023	-15.01	-0.73	8.34	-2.00
02.06.2023	-1.84	-0.83	-2.58	0.70
13.06.2023	-10.47	0.93	0.63	-0.19
15.06.2023	-8.19	1.80	2.09	-0.61
22.06.2023	-7.32	1.53	2.01	-0.58
30.06.2023	-4.04	1.99	1.44	-0.47
Absolute mean	8.53	1.32	2.63	0.71

Spike recovery

Spike recovery was measured during three runs at different dilution factors with the Sigma-Aldrich EOK. Each run consisted of nine samples, with three different spike concentrations of oxalic acid, analysed in triplicate. By calculating the average for every spike concentration at the three dilution factors, an average data row consisting of nine values is obtained. With a mean of 60.86 % (median = 57.94 %) the overall spike recovery lies below 80 % and is thus unsatisfactory. The recoveries range from 40 % to 85 % (Fig. 12), indicating a large variability (standard deviation (SD) = 13.12, RSD = 21.54 %). These findings suggest that the spike recovery is insufficient, not robust and unreliable.

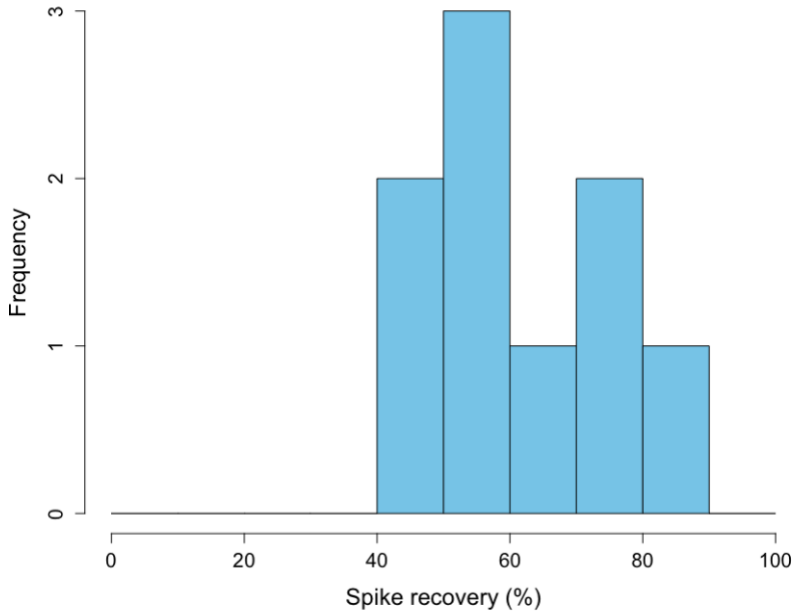

Fig. 12: Distribution of spike recoveries (%) obtained with the Sigma-Aldrich EOK

Repeatability

Since only spiked quartz sand samples were analysed in this study with the Sigma-Aldrich EOK, the results obtained with the Biotech Trinity EOK were used to test for repeatability (Rowley et al., In prep.). To do so, 13 plant samples were extracted and measured as replicates. Their CaOx content (%) was compared by calculating the percentual difference between the two replicates. On average, a difference of 32.55 % (median 23.00 %) can be observed, suggesting an insufficient repeatability. Ranging between 1 and 100 %, these differences exhibit large variability (Fig. 13; SD = 37.23, RSD = 87.44 %). Therefore, these findings suggest that the EOK has a very limited repeatability.

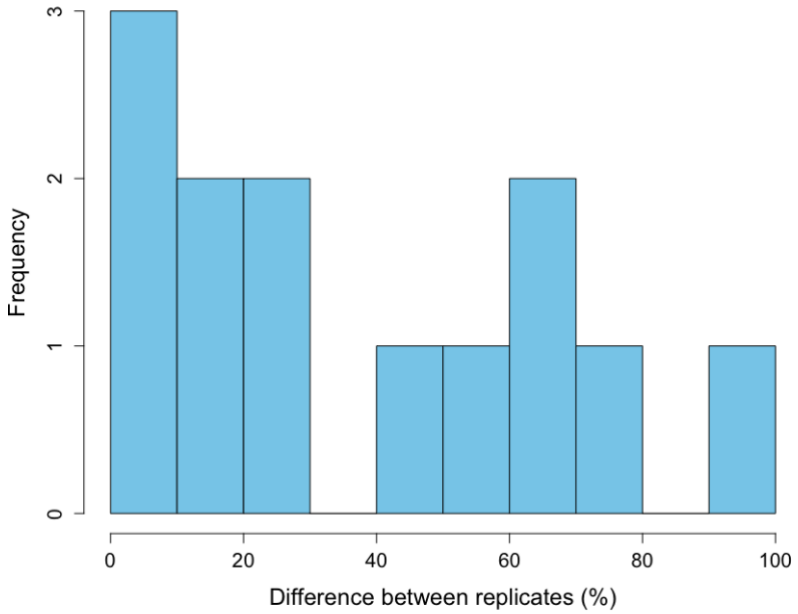

Fig. 13: Distribution of replicate differences (%) obtained with the Biotech Trinity EOK

Costs and time expenditure

The estimated cost for the complete extraction process and quantification using the Sigma-Aldrich EOK is approximately 80 CHF per sample, when run in duplicate. In contrast, using the Biotech Trinity EOK reduces the cost to approximately 30 – 50 CHF per sample, also run in duplicate. The extraction and sample preparation steps, such as pH adjustment and well plate setup, together with the EOK analysis take about 24 hours to complete for 30 – 40 samples. Notably, adjusting the pH of each sample is the most time-consuming step of the procedure.

4.3 High-performance liquid chromatography results

Linearity

Table 12 presents the slope, intercept, y value at x_{max} and the R^2 of the standard curves at the beginning (1st standard) and at the end (2nd standard) of each HPLC sequence. The R^2 values are all great, indicating a good linear model fit. This is the case for standards at the beginning and at the end of each run and therefore no intra method shift can be observed based on the R^2 values. The slope and y values at x_{max} show slight differences within their respective group. Interestingly, these differences decrease within the run and the values show a higher similarity in the second standards, suggesting that the measurements become more rugged. This pattern can be observed to some extent by looking at the intercept values which show the highest variability out of all four parameters.

The COV model values of the first standard (Tab. 13) and second standard (Tab. 14) reveal that the model fit is the worst at lower standards. At 0.5 mg/L, 2 mg/L standard and mostly 5 mg/L concentration the values are above the desired 5 %. At 20 mg/L the values show a sufficient model fit. This can also be observed for the second standard. However, the three lowest standards show a slightly better model fit when measured at the end of the run. Especially in the COV model of the second standards the bad model fit of the standards measured the 8th of October are striking. This can also be noticed to some extent by looking at the calibration parameters in Tab. 11.

Overall, the calibration curves of the newly developed method show a great and rugged linearity between and withing runs.

Tab. 12: Evaluation parameters of different calibration curves of the 1st and 2nd standard runs obtained with the final HPLC method

Date of measurement	1st standard				2nd standard			
	m	b	y at x_{max}	R^2	m	b	y at x_{max}	R^2
11.09.2024	38.36	8.82	12283.46	0.99996	-	-	-	-
18.09.2024	38.16	13.05	12225.74	0.99992	38.31	15.29	12275.47	0.99990
23.09.2024	32.52	-56.63	10350.52	0.99954	38.57	13.91	12355.50	0.99987
25.09.2024	26.51	-9.55	8473.85	0.99918	38.77	-0.26	12405.48	0.99995
30.09.2024	32.72	-6.49	10463.03	0.99980	38.48	-9.98	12304.72	0.99997
08.10.2024	36.02	27.84	11553.62	0.99959	33.56	114.87	10855.09	0.99639
22.10.2024	38.00	4.88	12165.60	0.99995	38.36	27.67	12301.92	0.99988
28.10.2024	38.28	40.68	12290.55	0.99996	38.27	43.79	12289.50	0.99981
30.10.2024	38.49	29.33	12346.49	0.99993	38.31	11.32	12269.14	0.99997
Absolute mean	35.45	21.92	11350.32	0.99976	37.83	29.64	12132.10	0.99947
Relative standard deviation (%)	11.62	81.91	11.77	0.027	4.58	124.35	4.27	0.12

Tab. 13: COV models at different standard concentrations of the 1st standard run obtained with the final HPLC method

Date of measurement	Concentrations of 1st standard run (mg/L)							
	0.5	**2**	**5**	**20**	**40**	**80**	**160**	**320**
11.09.2024	-55.62	-18.01	-10.50	-1.39	0.90	1.62	0.44	-0.22
18.09.2024	-82.87	-28.80	-9.82	-2.19	0.36	2.41	0.81	-0.35
23.09.2024	300.07	68.85	21.57	-4.18	-2.75	-2.98	-2.67	0.90
25.09.2024	300.00	69.00	21.60	-4.20	-2.75	-2.97	-2.67	0.90
30.09.2024	-12.74	-44.64	-21.96	5.08	5.60	0.68	-1.68	0.32
08.10.2024	-171.97	-59.33	-16.01	0.89	4.25	-0.93	3.13	-0.79
22.10.2024	-42.66	-13.36	-14.46	-2.18	0.32	1.88	0.61	-0.26
28.10.2024	88.65	-9.12	-6.82	-0.60	0.20	1.41	0.42	-0.19
30.10.2024	94.86	-38.41	-1.57	-2.13	-0.17	1.35	0.97	-0.32
Absolute mean	118.60	35.67	12.73	2.30	1.88	1.54	1.42	0.43

Tab. 14: COV models at different standard concentrations of the 2nd standard run obtained with the final HPLC method

Date of measurement	Concentrations of 2nd standard run (mg/L)							
	0.5	**2**	**5**	**20**	**40**	**80**	**160**	**320**
11.09.2024	-	-	-	-	-	-	-	-
18.09.2024	-102.91	-24.86	-12.32	-1.46	0.34	2.03	1.18	-0.42
23.09.2024	-81.23	-22.09	-12.20	-3.30	-0.02	2.15	1.43	-0.47
25.09.2024	-82.00	-22.00	-12.20	-3.30	-0.02	2.15	1.43	-0.47
30.09.2024	39.12	0.44	-9.07	4.23	0.13	0.42	0.60	-0.16
08.10.2024	-690.35	-178.20	-65.05	-4.02	5.02	11.35	7.25	-2.56
22.10.2024	-144.70	-1.16	-4.53	-0.84	-0.92	1.59	1.52	-0.46
28.10.2024	-165.36	-18.69	-2.99	-1.98	0.16	2.31	1.77	-0.58
30.10.2024	77.33	22.34	-9.77	-2.24	0.60	0.97	-0.53	0.07
Absolute mean	172.88	36.22	16.02	2.67	0.90	2.87	1.96	0.65

Limit of quantification

Limit of quantification (LOQ) refers to the upper and lower standard concentration until, which the amount of oxalate can be quantified reliably. For assessing the lower limit of quantification, the smallest oxalic acid standard concentration at which a peak is observable is used. In this case, the 0.5 mg/L oxalic acid standard. The upper limit of quantification is simply the highest standard concentration of the calibration curve, which is the 320 mg/L standard.

Spike recovery

Spike recovery was assessed by measuring a blank sample, spiked with oxalic acid, during seven of the nine runs. On average, 75.72 % of the added spike was recovered, which is not great but close to the desired threshold of 80 % and thus acceptable. However, with a median of 67.22 %, an SD of 17.04 % and an RSD of 22.50 % the shows a large variability. By visualising the results (Fig. 14) this can be confirmed, and a clear pattern is noticeable. Ranging between about 55 % and 70 %, the first four spike recoveries are very low and not sufficient. However, after the 8th of October an abrupt shift was observable and recoveries above 90 % were measured, which is excellent. It is therefore suggested that this observation does not depend on spike recovery and another factor is very likely to be the explanation. Consequently, spike recovery of the new method is considered to be very good.

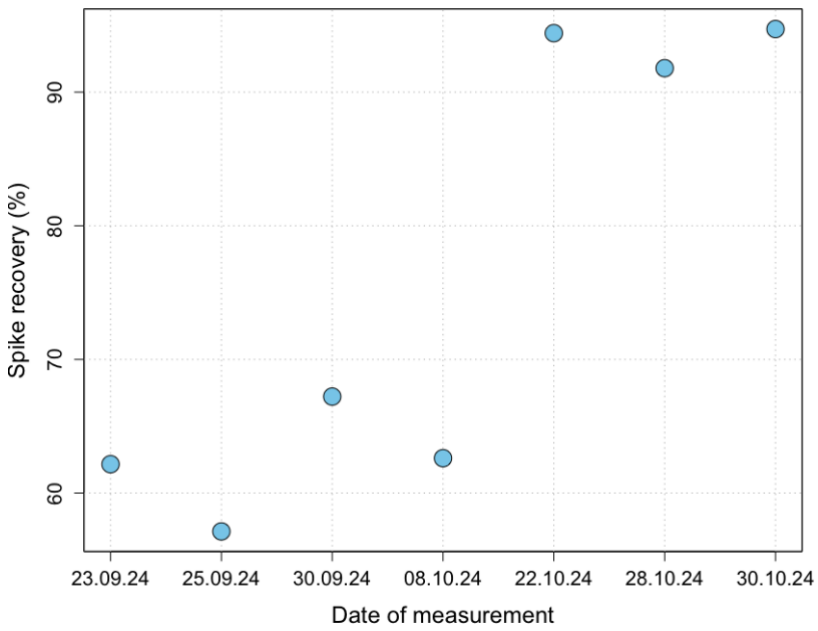

Fig. 14: Spike recoveries (%) of a spiked blank sample, measured across seven HPLC runs

Spike recovery was also determined for three plant and soil samples that were spiked with oxalic acid before extraction (Fig. 15). With a mean of 93.33 % the recovery of the plant samples is higher and its variability (SD = 10.53 %, RSD = 11.28 %) is lower compared to the soil samples. They recover 84.12 % on average and show a higher variability (SD = 28.81 %, RSD = 34.25 %).

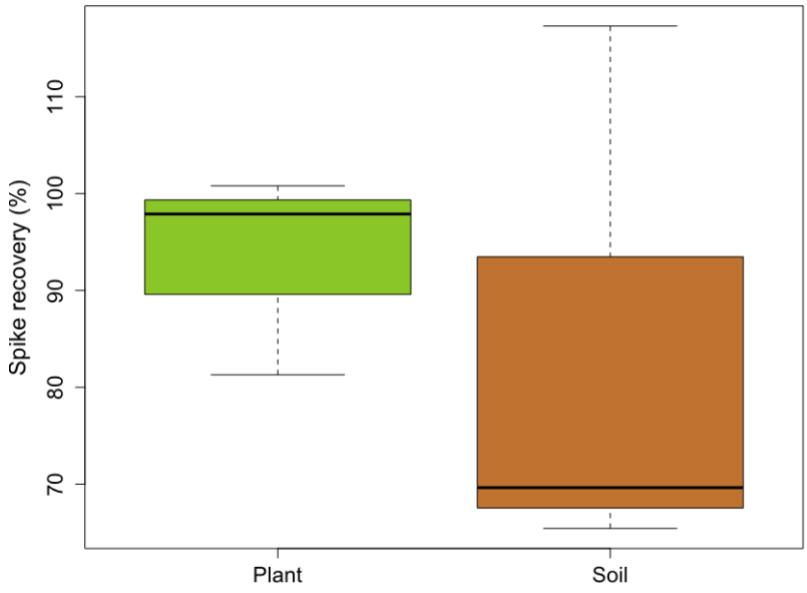

Fig. 15: Boxplot for the comparison of spike recovery of a plant and soil sample

Repeatability

In total, a set of 20 samples, consisting of eight plant and twelve soil samples, were extracted and measured twice, and their percentual difference was calculated to test for repeatability. On average, the overall difference is 30.74 %. Since the samples were now extracted in several steps, an acceptable difference between replicates lies in the range of 20 % - 30 %. Therefore, the results are acceptable. The median lies at 29.55 % in the same range. However, with an SD of 22.67 %, the RSD is 73.75 % the variability is rather high.

By analysing the distributions of the plant and soil samples separately (Fig. 16, B and C) the repeatability can be further investigated. A very high variability can be registered in the distribution of the plant samples (SD = 29.50 %, RSD = 100.36 %). Nevertheless, the results are either at the low or high end of the spectrum leading to a reasonable mean of 29.39 % and median of 15.29 % (Fig. 16, A). Soil samples are distributed more evenly over a similar range (Fig. 16, C) leading to a larger mean of 31.64 % (median = 33.47 %) and a smaller variability (SD = 18.22 %, RSD = 57.58 %).

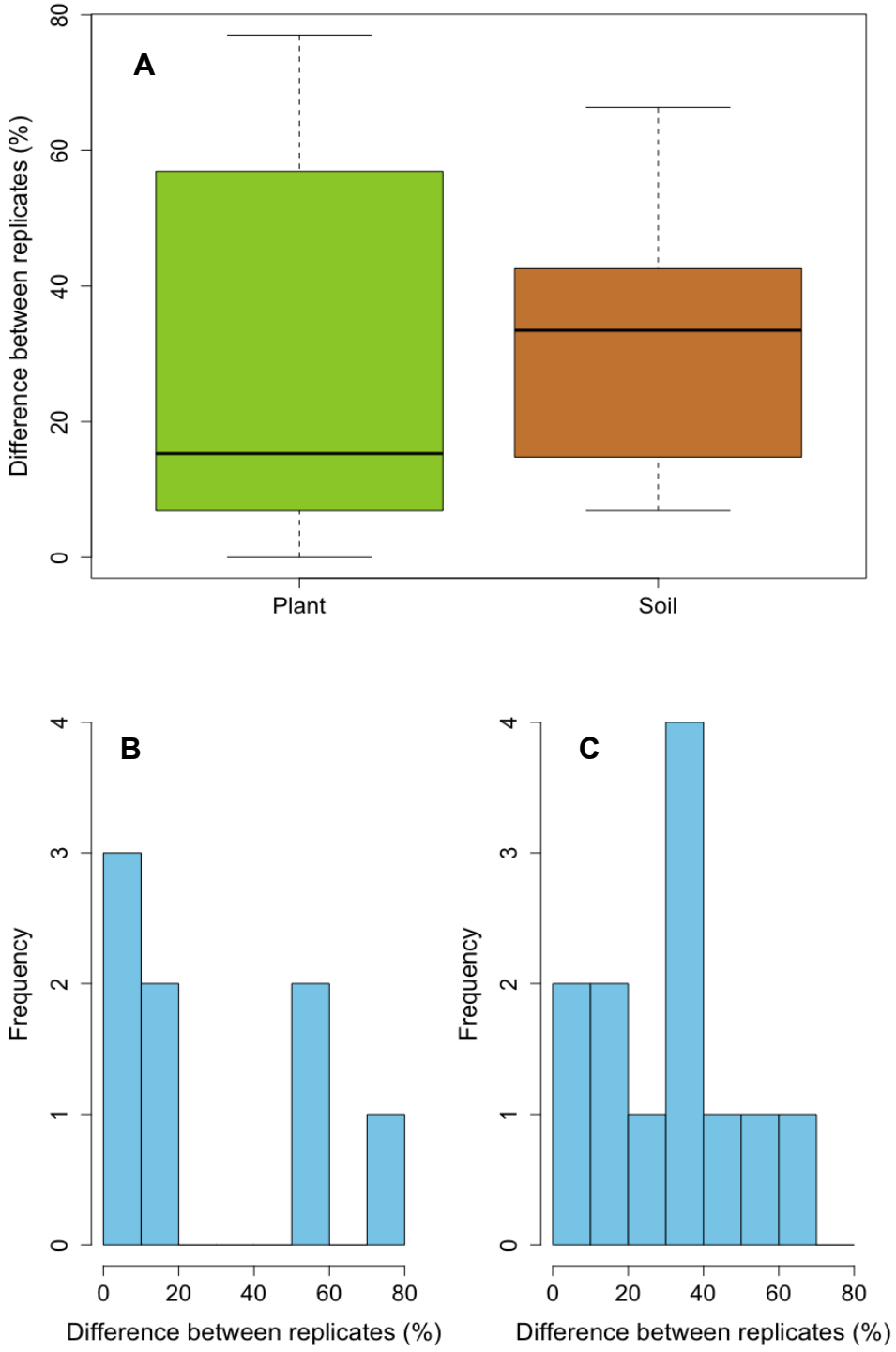

Fig. 16: Boxplot for the comparison of the repeatability of plant and soil samples (A) and distribution of differences of plant (B) and soil samples replicates (C)

Sample stability

To check for potential sample degradation over time, a random plant and soil sample that were prepared the 21st of August and stored at 3 °C in the fridge, were measured during seven of the nine runs. The sample stability was assessed by comparing the CaOx content. For the plant sample (Fig. 17) two groups can be identified: The first four samples show rather low and randomly distributed amounts of CaOx. Especially the low CaOx content of the second measurement is striking. The last three measurements are the highest and very similar. By looking at the soil samples (Fig. 18), the same pattern with two groups can be identified. The first four samples are again much smaller and more randomly distributed than the last three ones. However, the dip in the second measurement disappeared and the difference between the two groups is larger compared to the plant samples. Further, an increase of the CaOx content of the very last sample is noticeable. These findings thus propose a high sample stability over time since no degradation could be observed. Nonetheless, the similarity between the patterns of two randomly chosen samples is striking, suggesting that an external factor is responsible for the observed results. This assumption is also supported by the spike recovery results that showed the same pattern.

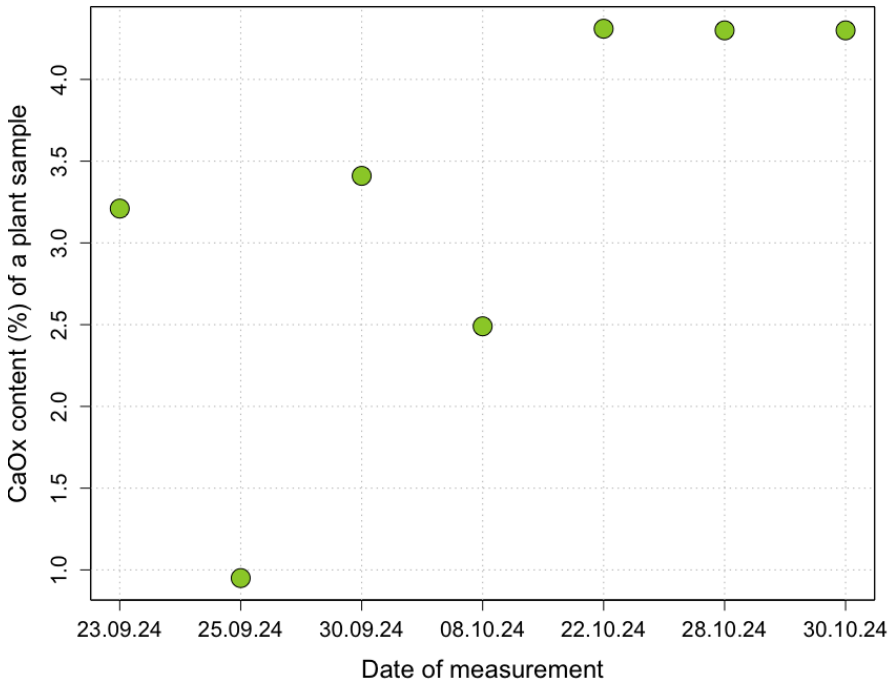

Fig. 17: CaOx contents (%) of a plant sample, measured across seven HPLC runs

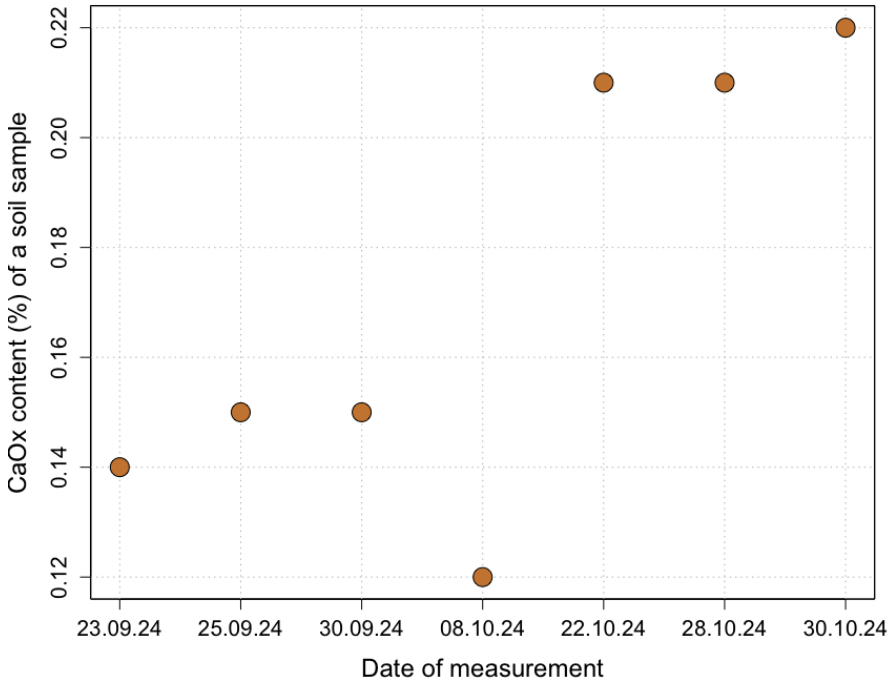

Fig. 18: CaOx contents (%) of a soil sample adjacent to the oxalic species, measured across seven HPLC runs

Costs and time expenditure

Analysing one sample in duplicate with the newly developed method costs approximately 45 CHF in total. The extraction step accounts for about 10 CHF, while the quantification with HPLC is in the range of 35 CHF.

The extraction and preparation of 20 samples, including filtration and dilution, takes about one and a half days. Analysing the samples, along with a set of 10 standards at the beginning and end of the run, requires about 35 hours.

5 Discussion

5.1 Method comparison

Results obtained with the EOK and the newly developed HPLC method are compared concerning the previously discussed validation criteria, i.e., linearity of the standard curve, spike recovery and extraction efficiency, repeatability, costs, and practicability to evaluate if the newly developed HPLC method can replace the commercial EOK. Furthermore, the newly developed method is compared to other HPLC protocols found in the literature.

Linearity

With a mean R^2 of 0.71, the linearity of the Sigma-Aldrich EOK is low and not comparable to the Biotech Trinity EOK and HPLC analysis. Both methods showed an overall $R^2 \geq 0.999$, which suggests a great linearity. Moreover, the linearity of the new HPLC method is comparable to HPLC methods developed in other studies (Arnetoli et al., 2008; Ding et al., 2006; Shen et al., 2021). R^2 values with an RSD ≤ 0.13 % between standard curves of the Biotech Trinity EOK and the HPLC method, indicate a great reliability. In contrast, with R^2 values ranging between 0.0254 and 0.998 and an RSD of about 60 % the Sigma-Aldrich EOK provides unreliable results. This finding is in line with the results of other linear regression parameters. RSD values for slope, intercept and endpoint varied in the case of the Sigma-Aldrich EOK between 60 % and 185 % between different calibration curves, whereas those values were similar for Biotech Trinity EOK and HPLC analysis. RSD values of slope and endpoint values across standard curves ranged between 8 and 9 % for the Biotech Trinity EOK and 4 and 11 % for the HPLC method. However, both EOK methods and the HPLC analysis showed the largest difference for the intercept. By looking at the COV model results for each standard concentration, the general key findings can be confirmed. The Sigma-Aldrich EOK shows a bad model fit and large variety between standard curves, whereas the Biotech Trinity EOK and HPLC method have lower COV model values indicating a good model fit. However, quantification with HPLC indicates a better model fit at low concentrations with less variability than the Biotech Trinity EOK, suggesting a more precise quantification at low concentrations. COV values lie in range with the results of the study by Shen et al. (2021) and lower COV values than the study by Maalouf et al. (2011). In summary, the linearity of the Biotech Trinity EOK and HPLC method is great and comparable, whereas the linearity of the Sigma-Aldrich EOK is insufficient.

Spike recovery

On average, the new extraction procedure yielded about 75 % spike recovery of spiked blank samples, which is 15 % higher than that of the old extraction method (Fig. 19). Two reasons are responsible for this increase. The first one is the sequential extraction. By adding two more extraction steps to the procedure, about 30 % more CaOx could be extracted, indicating that a single-step extraction used in combination with the EOK is not sufficient. Various other studies have shown that extending the extraction procedure to two or even more steps results in a higher yield of the target compound (Marillán & Uquiche, 2023; Maumela et al., 2020) . Another reason for an improved extraction efficiency is the use of a higher molarity of the acid which was also observed by Wu et al., (2009), among others.

However, compared to other studies, the average spike recovery of about 60 % for the Sigma-Aldrich EOK and 75 % for the HPLC is rather low. Maalouf et al. (2011) assessed recoveries ranging between 96.8 % and 106.7 % with the Biotech Trinity EOK for a 10 mg/L oxalate standard. The study conducted by Starkey & Fry (1993) obtained recoveries between 100 % and 102 % with an EOK by Sigma-Aldrich and 97 % - 100 % of spike recovery for their HPLC method. Other HPLC methods showed spike recoveries of about 80 and 103 %, depending on concentration, of the standard (Shen et al., 2021). This suggests that, in terms of spike recovery, the new extraction method in combination with the quantification by HPLC is underperforming. This is surprising because during the method development process, spike recovery of the new extraction method was great with > 85 %. Nonetheless, looking only at the average or median recovery does not tell the whole story. Going back to figure 19, it is noticeable that the variability of spike recoveries of the new method is larger than for the Sigma-Aldrich EOK. In the method validation, it was assessed that the spike recoveries of the Sigma-Aldrich EOK were rather randomly distributed without any pattern, suggesting a low reliability and arbitrariness of the method. The spike recoveries of the HPLC method, on the other hand, showed a pattern that leads to the conclusion of an inter-method shift of the HPLC device and not a method inaccuracy. By looking at the last three measurements, the spike recovery is above 90 %, which is a great result and is in line with the values provided by the literature.

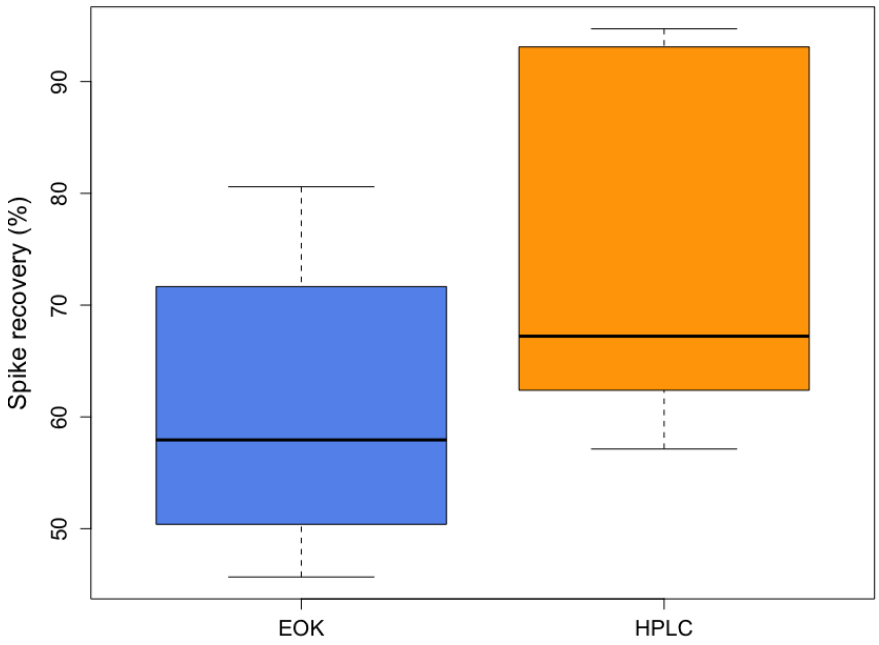

Fig. 19: Boxplot for the comparison of spike recovery of the Sigma-Aldrich EOK and the HPLC method

Extraction efficiency and sensitivity

Looking at spiked blank samples gives a good first overview of the extraction efficiency. However, the methods are designed for actual organic matter (and soil) samples and should therefore be tested how efficiently they extract the target compound in a complex matrix of actual samples. To do so, the CaOx contents of organic matter samples measured with the Biotech Trinity EOK and HPLC methods are compared (Fig. 20), the exact values can be found in appendix C, table 17 (plant) and 18 (soil). Since the EOK could not analyse the low CaOx content of soil samples due to its low sensitivity, only plant samples can be included in the comparison. The vast majority of measurements are located above the 1:1 line, indicating a higher extraction efficiency of the new method and confirming the findings of the spike recovery results. By adding more steps to the procedure and extraction with a stronger acid, the procedure could be optimised. Only two samples are located distinctively below the line. Additionally, the HPLC method allows for a more sensitive quantification than the Biotech Trinity EOK. This increased sensitivity of the HPLC method compared to the Biotech Trinity EOK was also found by Jordan et al. (1996). For both the spiked blank sample and especially the comparison of actual plant samples, the newly developed extraction and HPLC quantification method showed a higher extraction efficiency and sensitivity. Thus, optimisation for these criteria had been successful.

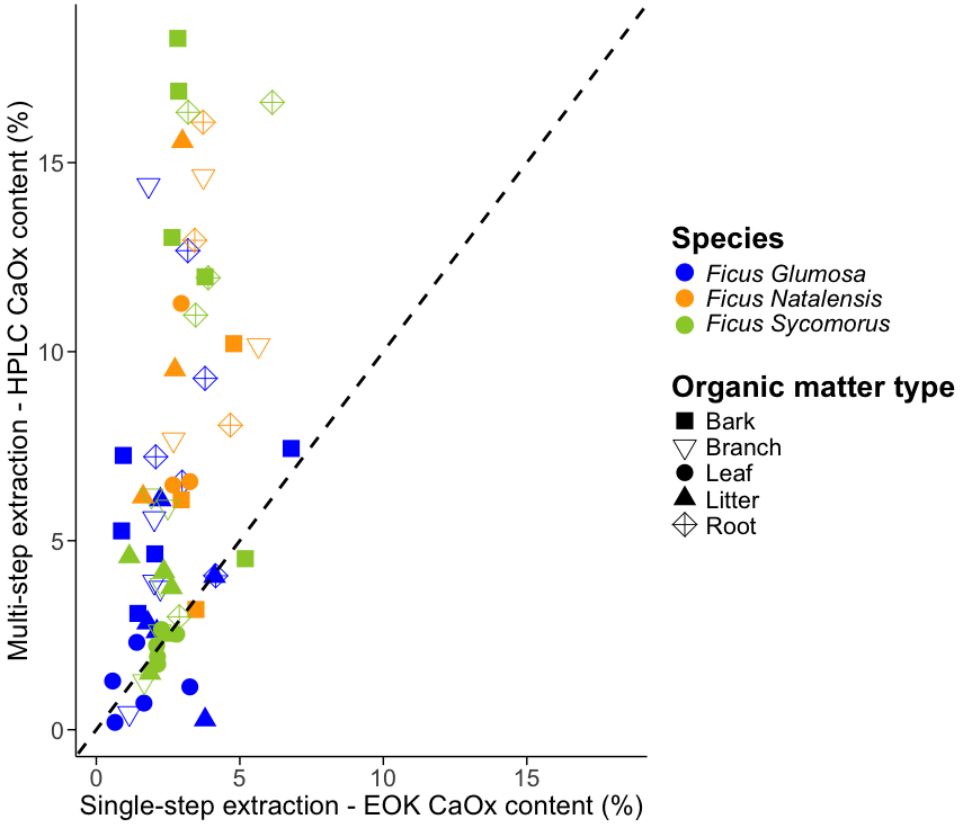

Fig. 20: Comparison of the obtained CaOx content (%) with the established extraction procedure in combination with the EOK and the new extraction method in combination with HPLC

Excursus: CaOx content of different organic matter types

Coming back to figure 20, each of the three analysed species is depicted in another colour, increasing the grade of information. Samples of *Ficus Glumosa* show the smallest increase in CaOx when measured with the new method. *Ficus Natalensis* and *Ficus Sycomorus* both showed a similar increase in CaOx content by applying the new extraction and HPLC method. However, the organic matter samples belonging to *Ficus Glumosa* were measured before the previously described inter-method shift, resulting in a sudden increase in spike recoveries and CaOx content of two samples by 30 – 50 %. *Ficus Natalensis* and *Ficus Sycomorus* were measured afterwards. The lower concentration of CaOx is thus more likely related to a skewed measurement than a difference between plant species, and thus this finding should be treated with caution.

Each shape in the graph corresponds to an organic matter type. Since they were not grouped by runs like the plant species, but mixed up, the method shift only applies to a limited extent, and statements can be made. Root samples showed the highest increase in extraction efficiency. Also, bark and branch samples seemed to be analysed more accurately with the new method. The smallest difference between the results of the EOK and HPLC method can be found for litter and especially leaf

samples. This finding can be explained by the overall distribution of oxalic acid in plant tissues. Leaf samples show the highest oxalic acid concentration while it is the lowest in roots (Çalişkan, 2000). Observing a strong increase in oxalate in root samples by analysing them with the new method indicates a higher extraction efficiency and sensitivity of the new method. Due to the high concentration of oxalic acid in the leaf samples the single-step extraction was already sufficient and only small increases in CaOx yield can be observed.

Repeatability

The replicate differences of the Biotech Trinity EOK and HPLC method were compared to assess repeatability (Fig. 21). With a median of 23 % for the Biotech Trinity EOK and 30.7 % for the HPLC method, the Biotech Trinity EOK method surprisingly shows a smaller difference between replicates and thus a better repeatability. In contrast, focusing on the means, which is 37.2 % for the EOK and 30.7 % for the HPLC method, suggests the opposite, concluding that repeatability is highly variable and slightly higher for the EOK. In the method validation section, a higher difference between replicates (20 – 30 %) for the HPLC than for the EOK (10 %) was observed because of the sequential extraction. Nonetheless, the optimisation process led to a decrease in variability. Interestingly, Maalouf et al. (2011) found a larger variability between HPLC replicates than between replicates measured with the Biotech Trinity EOK. However, the repeatability of the HPLC method is again partly biased due to the inter-method shift described earlier, which is discussed in more detail in section 5.2.

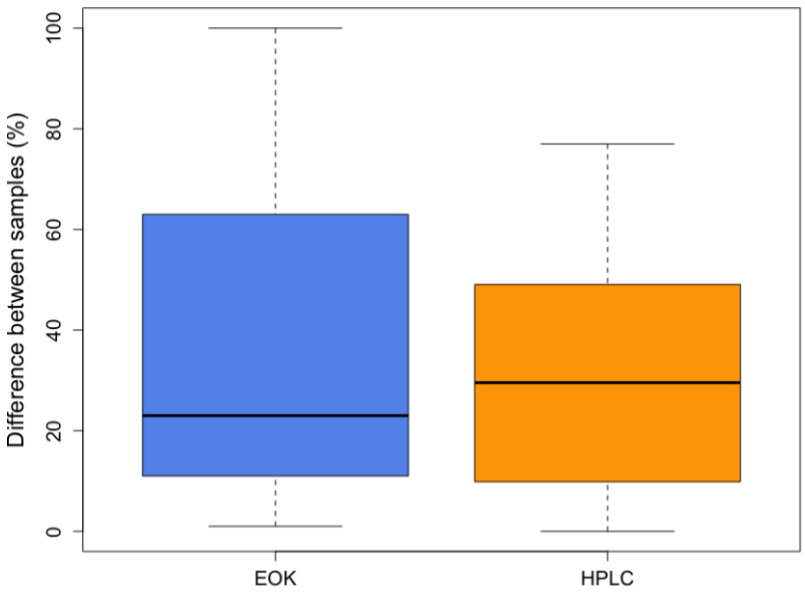

Fig. 21: Boxplot for comparison of the repeatability of the Biotech Trinity EOK and the HPLC method

Costs and time expenditure

Compared to the Sigma-Aldrich EOK, the costs of the HPLC method were almost cut in half. This was also observed in the study of Starkey & Fry (1993), where an even cheaper HPLC method was developed, which was only 28 % of the cost of the Sigma-Aldrich EOK. However, for the Biotech Trinity EOK, the expenses are similar to those of the newly developed method.

Extending the method by two additional extraction steps sample preparation takes a longer time compared to the EOK. However, the error-prone steps of adjusting the pH value and preparing the well plate can be avoided. Once developed, this makes the new method easier to apply.

Which method should be chosen?

Based on the compared criteria, the optimisation of the method has been successful, and the newly developed method has shown better performance. It shows a great linearity over a larger range with a higher sensitivity at low concentrations. Despite unsatisfying results for repeatability, it could be improved compared to the EOK analysis. The increased extraction efficiency led to a longer sample preparation process. Nevertheless, the procedure is more applicable due to the exclusion of error-prone steps. On top of that, the expenses of the method stayed in the same range. Therefore, the new extraction procedure in combination with HPLC quantification is preferable over the EOK method.

5.2 Limitations of the new method

Despite quantifying CaOx in plant and soil samples more precisely than the EOK, two main limitations of the newly developed method have to be pointed out.

The first limitation is an unknown compound in the soil sample, interfering with the CaOx peak in the chromatogram. While a single bell-shaped peak could be observed in the plant sample chromatogram, the chromatogram of the soil samples resulted in a double peak. The second peak could be clearly identified as oxalic acid. However, the compound responsible for the first peak remained unknown. Other studies quantifying oxalic acid in soil with HPLC did not observe this peak (Ding et al., 2006; Van Hees et al., 1999). In a first step, it was tested if the first peak is a different oxalate species which abundances are pH dependent (Simpson et al., 2009). Hence, three different samples with pH values of 3, 4-5 and 6-7 were prepared from the same soil sample extract that was used before. The chromatograms could not confirm that the unidentified peak refers to another oxalate species. A soil sample was spiked with CaOx, and the peak could be observed at the same retention time as oxalic acid. This

confirms that the unknown peak does not refer to another oxalate species. Another explanation of the unknown peak is the presence of other metals, such as Mg or iron (Fe), which can form complexes with oxalate (Strobel et al., 2004). Since such a complexation is more likely to occur in soil than in plants, it would explain why we only observe these two peaks in the soil chromatogram and not in the one of the plants. Ultimately, this is only speculation, and further investigation or method refinement is required.

The second limitation of the novel method is the potential inter-method shift mentioned a few times before. Between the 8th and 22nd of October a sudden increase by 20 % – 30 % in oxalate of three independent samples were measured by the HPLC. After this increase the last three measurements showed the same amount of oxalate. Since neither the samples nor the parameter settings and chemicals were changed in the meantime, it is most likely that the HPLC device is responsible for this observation. Therefore, this sudden increase in oxalate is most likely an inter-method shift. Between the shift sequences were stopped twice by the HPLC device due to detected leakage. After checking on the device, it could be ascertained that the signal was caused by condensation water and not an actual leak. A leak could influence the peak area (Meyer, 1997). Another option could be an injection issue (Raval & Patel, 2020). However, the exact reason for this shift remains unclear and might have been an individual case. Ultimately, these are minor limitations which do not prevent the new protocol from being a valuable and powerful tool for a more precise CaOx quantification.

5.3 Implications

Given the previously discussed limitations, the advantages of the new method outweigh the disadvantages, and a meaningful contribution is provided by this thesis. The method's applicability to both plant and, in contrast to the EOK, soil samples enables a deeper investigation of plant species with an active OCP and thus a better understanding of the underlying processes. By precisely analysing the amount of CaOx also in soil samples adjacent to an oxalogenic species, researchers are no longer restricted to the alkalinisation of acidic soils as a geochemical proxy or microscopy techniques to study the dynamics of oxalate in soils. By quantifying CaOx in situ, the newly developed method provides a reliable tool to expand CaOx studies to different environments, such as calcareous soil with a higher pH. This helps to better understand the complexity of the OCP (Rowley et al., 2017). These generated insights of the OCP allow an enhanced identification of the corresponding long-term C sinks, which have the potential to play an important role in regulating CO_2^{Atm} and thus mitigate climate change (Cailleau et al., 2005, 2014; Verrecchia et al., 2006).

6 Conclusions and outlook

This study aimed to develop and evaluate a new HPLC method for quantifying CaOx in the plant-soil system that is more precisely than commercial EOKs which are the established method. Method development optimised HPLC conditions, resulting in a mobile phase of 400 mM H_3PO_4 at 0.4 mL/min, two 150 mm C_{18} columns at 8 °C, and improved extraction using 2.5 M H_3PO_4 with two extra extraction steps (research question 1). Validation of the newly developed approach showed excellent linearity of the calibration curves, good spike recovery, and repeatability, confirming precision and reliability. Furthermore, the newly developed method successfully analysed plant and soil samples, as expected (research question 2). Compared to the standard EOK method, the novel approach delivered higher extraction efficiency, which is due to the addition of two extraction steps and the use of a stronger acid. Furthermore, the novel method offers a more precise, reliable and less costly quantification than the EOK and matched other reported HPLC protocols, which also meets the expectations (research question 3).

Despite these achievements and accomplishing the aim of this thesis, a few limitations remain. The appearance of a double peak in the chromatograms of soil samples indicates an incomplete separation with an unknown compound. Identifying the compound or refining the chromatographic conditions, such as column type, may help resolve this peak issue. Additionally, the "suspicious pattern" or unexplained shift observed in three unrelated samples suggests that there may be inter-method variability.

Nonetheless, the novel approach represents a step forward in CaOx quantification for both plant and especially soil matrices. This advancement has the potential to support a more comprehensive understanding of oxalate dynamics, the OCP and identifying associated long-term C sinks and offer a meaningful contribution in addressing the climate change problematic. By expanding the method to quantifying other low molecular weight organic acids besides oxalic acid, as already accomplished in other HPLC protocols (Ding et al., 2006; Van Hees et al., 1999), the applicability of the method could be broadened applied when applied to soils. Various soil properties and processes could be analysed by quantifying those compounds, such as soil health and fertility, carbon cycling and mobilisation of heavy metals and other soil pollutants (Sokolova, 2020). Therefore, the procedure developed in this thesis serves as a potential foundation for improving soil management practices and not only offers a powerful tool contributing to climate change mitigation.

Acknowledgements

I would like to thank all those who contributed to the completion of this thesis and supported me during this time.

First, I want to thank my supervisors, PD Dr. Guido L. B. Wiesenberg and Dr. Mike C. Rowley. Thank you for always guiding me, motivating me and supporting me. I really appreciate the time, patience, and energy you both invested in helping me get to the top of the mountain.

Special thanks to Yves Brügger and Barbara Siegfried, who made sure everything ran smoothly in the lab and that I had everything I needed for my lab work.

I also want to thank Binyan Sun for always being ready to offer help, encouragement or some fancy tea.

Thank you to everyone else in the 2B and GCH group for welcoming me and lending me a lab key so that I could actually get started in the morning.

Lastly, I want to thank my friends and family for always being there for me. I am especially grateful for my parents who made my studies possible and went through all kinds of emotions with me.

References

Abdu Hussen, A. (2022). High-Performance Liquid Chromatography (HPLC): A review. *Annals of Advances in Chemistry*, *6*(1), 010–020. https://doi.org/10.29328/journal.aac.1001026

Afsarimanesh, N., Mukhopadhyay, S. C., & Kruger, M. (2018). Sensing technologies for monitoring of bone-health: A review. *Sensors and Actuators, A: Physical*, *274*, 165–178. https://doi.org/10.1016/j.sna.2018.03.027

Álvarez-Rivera, O. O., Estrada-Medina, H., Jiménez-Osornio, J. J., O'Connor-Sánchez, I. A., Navarro-Alberto, J. A., Ferrer, M. M., Canto-Canché, B., & Tzec-Gamboa, M. del C. (2021). Differences in oxalate–carbonate pathway of Brosimum alicastrum in karst homegarden and forest soils. *Soil Science Society of America Journal*, *85*(3), 691–702. https://doi.org/10.1002/saj2.20228

Aragno, M., Verrecchia, E. P., Job, D., Cailleau, G., Braissant, O., Khammar, N., Ferro, K., Mota, M., Guggiari, M., & Martin, G. (2010). Calcium carbonate biomineralization in ferralitic, tropical soils through the oxalate-carbonate pathway. *BGS Bull*, 127–130.

Arnetoli, M., Montegrossi, G., Buccianti, A., & Gonnelli, C. (2008). Determination of organic acids in plants of silene paradoxa L. by HPLC. *Journal of Agricultural and Food Chemistry*, *56*(3), 789–795. https://doi.org/10.1021/jf072203d

Baldwin, J. W., Dessy, J. B., Vecchi, G. A., & Oppenheimer, M. (2019). Temporally Compound Heat Wave Events and Global Warming: An Emerging Hazard. *Earth's Future*, *7*(4), 411–427. https://doi.org/10.1029/2018EF000989

Barnosky, A. D., Koch, P. L., Feranec, R. S., Wing, S. L., & Shabel, A. B. (2004). Assessing the causes of late Pleistocene extinctions on the continents. *Science (New York, N.Y.)*, *306*(5693), 70–75. https://doi.org/10.1126/SCIENCE.1101476

Batjes, N. H. (1996). Total carbon and nitrogen in the soils of the world. *European Journal of Soil Science*, *47*(2), 151–163. https://doi.org/10.1111/j.1365-2389.1996.tb01386.x

Batool, M., Cihacek, L. J., & Alghamdi, R. S. (2024). Soil Inorganic Carbon Formation and the Sequestration of Secondary Carbonates in Global Carbon Pools: A Review. In *Soil Systems* (Vol. 8, Issue 1, p. 15). Multidisciplinary Digital Publishing Institute. https://doi.org/10.3390/soilsystems8010015

Braissant, O., Cailleau, G., Aragno, M., & Verrecchia, E. P. (2004). Biologically induced mineralization in the tree Milicia excelsa (Moraceae): its causes and consequences to the environment. *Geobiology*, *2*(1), 59–66. https://doi.org/10.1111/j.1472-4677.2004.00019.x

Braissant, O., Verrecchia, E. P., & Aragno, M. (2002). Is the contribution of bacteria to terrestrial carbon budget greatly underestimated? *Naturwissenschaften*, *89*(8), 366–370. https://doi.org/10.1007/s00114-002-0340-0

Bravo, D., Cailleau, G., Bindschedler, S., Simon, A., Job, D., Verrecchia, E., & Junier, P. (2013). Isolation of oxalotrophic bacteria able to disperse on fungal mycelium. *FEMS Microbiology Letters*, *348*(2), 157–166. https://doi.org/10.1111/1574-6968.12287

Cailleau, G., Braissant, O., & Verrecchia, E. P. (2011). Turning sunlight into stone: The oxalate-carbonate pathway in a tropical tree ecosystem. *Biogeosciences*, *8*(7), 1755–1767. https://doi.org/10.5194/bg-8-1755-2011

Cailleau, G., Braissant, O., Dupraz, C., Aragno, M., & Verrecchia, E. P. (2005). Biologically induced accumulations of $CaCO_3$ in orthox soils of Biga, Ivory Coast. *Catena*, *59*(1), 1–17. https://doi.org/10.1016/j.catena.2004.06.002

Cailleau, G., Braissant, O., & Verrecchia, E. P. (2004). Biomineralization in plants as a long-term carbon sink. *Naturwissenschaften*, *91*(4), 191–194. https://doi.org/10.1007/s00114-004-0512-1

Cailleau, G., Mota, M., Bindschedler, S., Junier, P., & Verrecchia, E. P. (2014). Detection of active oxalate-carbonate pathway ecosystems in the Amazon Basin: Global implications of a natural potential C sink. *Catena*, *116*, 132–141. https://doi.org/10.1016/j.catena.2013.12.017

Çalişkan, M. (2000). The metabolism of oxalic acid. *Turkish Journal of Zoology*, *24*(1), 103–106.

Cannon, J. P., Allen, E. B., Allen, M. F., Dudley, L. M., & Jurinak, J. J. (1995). The effects of oxalates produced by Salsola tragus on the phosphorus nutrition of Stipa pulchra. *Oecologia*, *102*(3), 265–272. https://doi.org/10.1007/BF00329792

Castellari, M., Versari, A., Spinabelli, U., Galassi, S., & Amati, A. (2000). An improved HPLC method for the analysis of organic acids, carbohydrates, and alcohols in grape musts and wines. *Journal of Liquid Chromatography and Related Technologies*, *23*(13), 2047–2056. https://doi.org/10.1081/JLC-100100472

Certini, G., Corti, G., & Ugolini, F. C. (2000). Vertical trends of oxalate concentration in two soils under Abies alba from Tuscany (Italy). *Journal of Plant Nutrition and Soil Science*, *163*(2), 173–177. https://doi.org/10.1002/(SICI)1522-2624(200004)163:2<173::AID-JPLN173>3.0.CO;2-H

Chabbi, A., Lehmann, J., Ciais, P., Loescher, H. W., Cotrufo, M. F., Don, A., Sanclements, M., Schipper, L., Six, J., Smith, P., & Rumpel, C. (2017). Aligning agriculture and climate policy. In *Nature Climate Change, 7*(5), 307–309. https://doi.org/10.1038/nclimate3286

Cowan, D. A., Babenko, D., Bird, R., Botha, A., Breecker, D. O., Clarke, C. E., Francis, M. L., Gallagher, T., Lebre, P. H., Nel, T., Potts, A. J., Trindade, M., & Van Zyl, L. (2024). Oxalate and oxalotrophy: an environmental perspective. *Sustainable Microbiology*, *1*(1), 4. https://doi.org/10.1093/sumbio/qvad004

Ding, J., Wang, X., Zhang, T., Li, Q., & Luo, M. (2006). Optimization of RP-HPLC analysis of low molecular weight organic acids in soil. *Journal of Liquid Chromatography and Related Technologies*, *29*(1), 99–111. https://doi.org/10.1080/10826070500363050

Erickson, L. E. (2017). Reducing greenhouse gas emissions and improving air quality: Two global challenges. *Environmental Progress & Sustainable Energy*, *36*(4), 982–988. https://doi.org/10.1002/EP.12665

Esri. "World Imagery" [basemap]. Scale Not Given. "ArcGIS online". November 07, 2024. https://www.arcgis.com/home/item.html?id=10df2279f9684e4a9f6a7f08febac2a9. (22.03.2025).

Eswaran, H., Reich, P. H., Kimble, J. M., Beinroth, F. H., Padmanabhan, E., & Moncharoen, P. (2000). Global carbon stock. *Global Climate Change and Pedogenic Carbonates*, 15–25. https://doi.org/10.14962/JASS.20.2_168

Franceschi, V. R., & Nakata, P. A. (2005). Calcium oxalate in plants: Formation and function. In *Annual Review of Plant Biology, 56*, 41–71. Annu Rev Plant Biol. https://doi.org/10.1146/annurev.arplant.56.032604.144106

Fuss, S., Lamb, W. F., Callaghan, M. W., Hilaire, J., Creutzig, F., Amann, T., Beringer, T., De Oliveira Garcia, W., Hartmann, J., Khanna, T., Luderer, G., Nemet, G. F., Rogelj, J., Smith, P., Vicente, J. V., Wilcox, J., Del Mar Zamora Dominguez, M., & Minx, J. C. (2018). Negative emissions - Part 2: Costs, potentials and side effects. In *Environmental Research Letters, 13*(6). IOP Publishing. https://doi.org/10.1088/1748-9326/aabf9f

Gerke, J. (2022). The Central Role of Soil Organic Matter in Soil Fertility and Carbon Storage. In *Soil Systems, 6*(2), 33. Multidisciplinary Digital Publishing Institute. https://doi.org/10.3390/soilsystems6020033

Gómez, I. B., Ramos, M. J. G., Rajski, Ł., Flores, J. M., Jesús, F., & Fernández-Alba, A. R. (2022). Ion chromatography coupled to Q-Orbitrap for the analysis of formic and oxalic acid in beehive matrices: a field study. *Analytical and Bioanalytical Chemistry*, *414*(7), 2419–2430. https://doi.org/10.1007/s00216-022-03882-2

Hansen, E. H., Winther, S. K., & Gundstrup, M. (1994). Enzymatic assay of oxalate in urine by flow injection analysis using immobilized oxalate oxidase and chemiluminescence detection. *Analytical Letters*, *27*(7), 1239–1253. https://doi.org/10.1080/00032719408006365

Heimann, M., & Reichstein, M. (2008). Terrestrial ecosystem carbon dynamics and climate feedbacks. *Nature*, *451*(7176), 289–292. https://doi.org/10.1038/nature06591

Hönow, R., & Hesse, A. (2002). Comparison of extraction methods for the determination of soluble and total oxalate in foods by HPLC-enzyme-reactor. *Food Chemistry*, *78*(4), 511–521. https://doi.org/10.1016/S0308-8146(02)00212-1

Hunt, C., Kenealy, W., Horn, E., & Houtman, C. (2004). A biopulping mechanism: Creation of acid groups on fiber. *Holzforschung*, *58*(4), 434–439. https://doi.org/10.1515/HF.2004.066

IPCC. (2023). Climate Change 2023: Synthesis Report. A Report of the Intergovernmental Panel on Climate Change. In *Diriba Korecha Dadi*. https://doi.org/10.59327/IPCC/AR6-9789291691647

Jaureguiberry, P., Titeux, N., Wiemers, M., Bowler, D. E., Coscieme, L., Golden, A. S., Guerra, C. A., Jacob, U., Takahashi, Y., Settele, J., Díaz, S., Molnár, Z., & Purvis, A. (2022). The direct drivers of recent global anthropogenic biodiversity loss. *Science Advances*, *8*(45), 9982. https://doi.org/10.1126/SCIADV.ABM9982/SUPPL_FILE/SCIADV.ABM9982_DATA_S1.ZIP

Jayasuriya, G. C. (1955). The isolation and characteristics of an oxalate-decomposing organism. *Journal of General Microbiology*, *12*(3), 419–428. https://doi.org/10.1099/00221287-12-3-419

Jobbágy, E. G., & Jackson, R. B. (2001). The distribution of soil nutrients with depth: Global patterns and the imprint of plants. *Biogeochemistry*, *53*(1), 51–77. https://doi.org/10.1023/A:1010760720215

Jordan, C. R., Dashek, W. V., & Highley, T. L. (1996). Detection and quantification of oxalic acid from the brown-rot decay fungus, Postia placenta. *Holzforschung*, *50*(4), 312–318. https://doi.org/10.1515/hfsg.1996.50.4.312

Judd, E. J., Tierney, J. E., Lunt, D. J., Montañez, I. P., Huber, B. T., Wing, S. L., & Valdes, P. J. (2024). A 485-million-year history of Earth ' s surface temperature. *Science*, *385*(6715). https://doi.org/10.1126/science.adk3705

Junier, P., Cailleau, G., Palmieri, I., Vallotton, C., Trautschold, O. C., Junier, T., Paul, C., Bregnard, D., Palmieri, F., Estoppey, A., Buffi, M., Lohberger, A., Robinson, A., Kelliher, J. M., Davenport, K., House, G. L., Morales, D., Gallegos-Graves, L. V., Dichosa, A. E. K., … Chain, P. S. G. (2021). Democratization of fungal highway columns as a tool to investigate bacteria associated with soil fungi. *FEMS Microbiology Ecology*, *97*(2). https://doi.org/10.1093/femsec/fiab003

Kassa, A., Tadele, Y., & Mekasha, Y. (2015). Ficus sycomorus (Sycamore Fig or Shola) Leaf, A Potential Source of Protein for Ruminants: A Review. *Journal of Fisheries & Livestock Production*, *03*(04). https://doi.org/10.4172/2332-2608.1000152

Konno, K., Inoue, T. A., & Nakamura, M. (2014). Synergistic defensive function of raphides and protease through the needle effect. *PLoS ONE*, *9*(3), e91341. https://doi.org/10.1371/journal.pone.0091341

Kotani, A., Ishikawa, H., Shii, T., Kuroda, M., Mimaki, Y., Machida, K., Yamamoto, K., & Hakamata, H. (2023). Determination of oxalic acid in herbal medicines by semi-micro hydrophilic interaction liquid chromatography coupled with electrochemical detection. *Analytical Sciences*, *39*(4), 441–446. https://doi.org/10.1007/s44211-022-00245-w

L'Initiative internationale "4 pour 1000". (2015). *The international "4 per 1000" Initiative. Soils for Food Security and Climate*. https://4p1000.org/

Lal, R. (2004a). Soil carbon sequestration impacts on global climate change and food security. *Science*, *304*(5677), 1623–1627. https://doi.org/10.1126/SCIENCE.1097396/ASSET/8A21EF09-10F3-41F6-810F-1B286C8DA4E3/ASSETS/GRAPHIC/ZSE0230426030004.JPEG

Lal, R. (2004b). Agricultural activities and the global carbon cycle. *Nutrient Cycling in Agroecosystems*, *70*(2), 103–116. https://doi.org/10.1023/B:FRES.0000048480.24274.0f

Lehmann, J., & Kleber, M. (2015). The contentious nature of soil organic matter. In *Nature*, *528*(7580), 60–68. Nature Publishing Group. https://doi.org/10.1038/nature16069

Li, W., Zheng, J., Chen, M., Liu, B., Liu, Z., & Gong, L. (2022). Simultaneous determination of oxalate and citrate in urine and serum of calcium oxalate kidney stone rats by IP-RP LC-MS/MS. *Journal of Chromatography B: Analytical Technologies in the Biomedical and Life Sciences*, *1208*, 123395. https://doi.org/10.1016/j.jchromb.2022.123395

Liu, Z., Eden, J. M., Dieppois, B., & Blackett, M. (2022). A global view of observed changes in fire weather extremes: uncertainties and attribution to climate change. *Climatic Change*, *173*(1–2), 1–20. https://doi.org/10.1007/s10584-022-03409-9

Locatelli, M., Furton, K. G., Tartaglia, A., Sperandio, E., Ulusoy, H. I., & Kabir, A. (2019). An FPSE-HPLC-PDA method for rapid determination of solar UV filters in human whole blood, plasma and urine. *Journal of Chromatography B: Analytical Technologies in the Biomedical and Life Sciences*, *1118–1119*, 40–50. https://doi.org/10.1016/j.jchromb.2019.04.028

Maalouf, N. M., Adams Huet, B., Pasch, A., Lieske, J. C., Asplin, J. R., Siener, R., Hesse, A., Nuoffer, J. M., Frey, F. J., Knight, J., Holmes, R. P., Zerwekh, J. E., & Bonny, O. (2011). Variability in urinary oxalate measurements between six international laboratories. *Nephrology Dialysis Transplantation*, *26*(12), 3954–3959. https://doi.org/10.1093/ndt/gfr147

Marillán, C., & Uquiche, E. (2023). Extraction of bioactive compounds from Leptocarpha rivularis stems by three-stage sequential supercritical extraction in fixed bed extractor using CO_2 and ethanol-modified CO_2. *Journal of Supercritical Fluids*, *197*, 105903. https://doi.org/10.1016/j.supflu.2023.105903

Maumela, P., van Rensburg, E., Chimphango, A. F. A., & Görgens, J. F. (2020). Sequential extraction of protein and inulin from the tubers of Jerusalem artichoke (Helianthus tuberosus L.). *Journal of Food Science and Technology*, *57*(2), 775–786. https://doi.org/10.1007/s13197-019-04110-z

Meyer, V. R. (1997). Influence of leaks in the liquid chromatographic instrument on analytical results. *Journal of Chromatography A*, *767*(1–2), 25–31. https://doi.org/10.1016/S0021-9673(96)01096-5

Misiewicz, B., Mencer, D., Terzaghi, W., & VanWert, A. L. (2023). Analytical Methods for Oxalate Quantification: The Ubiquitous Organic Anion. *Molecules*, *28*(7). https://doi.org/10.3390/molecules28073206

Mohseni, N., & Salar, Y. S. (2021). Terrain indices control the quality of soil total carbon stock within water erosion-prone environments. *Ecohydrology and Hydrobiology*, *21*(1), 46–54. https://doi.org/10.1016/j.ecohyd.2020.08.006

Monje, P. V., & Baran, E. J. (2002). Characterization of calcium oxalates generated as biominerals in cacti. *Plant Physiology*, *128*(2), 707–713. https://doi.org/10.1104/pp.010630

Mu, Y., Wu, Y., Wang, X., Hu, L., & Ke, R. (2022). Determination of 10 organic acids in alcoholic products by ion chromatography-tandem mass spectrometry. *Chinese Journal of Chromatography (Se Pu)*, *40*(12), 1128–1135. https://doi.org/10.3724/SP.J.1123.2022.01020

Myhre, G., Alterskjær, K., Stjern, C. W., Hodnebrog, Marelle, L., Samset, B. H., Sillmann, J., Schaller, N., Fischer, E., Schulz, M., & Stohl, A. (2019). Frequency of extreme precipitation increases extensively with event rareness under global warming. *Scientific Reports*, *9*(1), 1–10. https://doi.org/10.1038/s41598-019-52277-4

Nair, P. K. R., Kumar, B. M., & Nair, V. D. (2022). An introduction to agroforestry: Four decades of scientific developments. In *An Introduction to Agroforestry: Four Decades of Scientific Developments*. Springer International Publishing. https://doi.org/10.1007/978-3-030-75358-0

Nakata, P. A. (2003). Advances in our understanding of calcium oxalate crystal formation and function in plants. In *Plant Science*, *164*(6), 901–909. Elsevier Ireland Ltd. https://doi.org/10.1016/S0168-9452(03)00120-1

Neukom, R., Barboza, L. A., Erb, M. P., Shi, F., Emile-Geay, J., Evans, M. N., Franke, J., Kaufman, D. S., Lücke, L., Rehfeld, K., Schurer, A., Zhu, F., Brönnimann, S., Hakim, G. J., Henley, B. J., Ljungqvist, F. C., McKay, N., Valler, V., & von Gunten, L. (2019). Consistent multidecadal variability in global temperature reconstructions and simulations over the Common Era. *Nature Geoscience*, *12*(8), 643–649. https://doi.org/10.1038/s41561-019-0400-0

Paiva, É. A. S. (2021). Do calcium oxalate crystals protect against herbivory? *Science of Nature*, *108*(3), 1–7. https://doi.org/10.1007/s00114-021-01735-z

Poulton, P., Johnston, J., Macdonald, A., White, R., & Powlson, D. (2018). Major limitations to achieving "4 per 1000" increases in soil organic carbon stock in temperate regions: Evidence from long-term experiments at Rothamsted Research, United Kingdom. *Global Change Biology*, *24*(6), 2563–2584. https://doi.org/10.1111/gcb.14066

Prentice, I., Farquhar, G., Fasham, M., Goulden, M., Heimann, M., Jaramillo, V., Kheshgi, H., Le Quéré, C., Scholes, R., & Wallace, D. (2001). The carbon cycle and atmospheric carbon dioxide. In *Climate Change 2001: The Scientific Basis* (pp. 183–237). Cambridge University Press. https://research-portal.uea.ac.uk/en/publications/the-carbon-cycle-and-atmospheric-carbon-dioxide

Raposo, F., & Ibelli-Bianco, C. (2020). Performance parameters for analytical method validation: Controversies and discrepancies among numerous guidelines. In *TrAC - Trends in Analytical Chemistry* (Vol. 129, p. 115913). Elsevier. https://doi.org/10.1016/j.trac.2020.115913

Raval, K., & Patel, H. (2020). Review on Common Observed HPLC Troubleshooting Problems. *International Journal of Pharma Research and Health Sciences*, *8*(4), 3195–3202. https://doi.org/10.21276/ijprhs.2020.04.02

Raza, S., Irshad, A., Margenot, A., Zamanian, K., Li, N., Ullah, S., Mehmood, K., Ajmal Khan, M., Siddique, N., Zhou, J., Mooney, S. J., Kurganova, I., Zhao, X., & Kuzyakov, Y. (2024). Inorganic carbon is overlooked in global soil carbon research: A bibliometric analysis. *Geoderma*, *443*, 116831. https://doi.org/10.1016/j.geoderma.2024.116831

Retallack, G. J. (Greg J. (1990). *Soils of the past : an introduction to paleopedology*. Unwin Hyman.

Rojas-Molina, I., Gutiérrez-Cortez, E., Bah, M., Rojas-Molina, A., Ibarra-Alvarado, C., Rivera-Muñoz, E., Del Real, A., & Aguilera-Barreiro, M. D. L. A. (2015). Characterization of calcium compounds in opuntia ficus indica as a source of calcium for human diet. *Journal of Chemistry*, *2015*(1), 710328. https://doi.org/10.1155/2015/710328

Rowley, M. C., Estrada-Medina, H., Tzec-Gamboa, M., Rozin, A., Cailleau, G., Verrecchia, E. P., & Green, I. (2017). Moving carbon between spheres, the potential oxalate-carbonate pathway of Brosimum alicastrum Sw.; Moraceae. *Plant and Soil*, *412*(1–2), 465–479. https://doi.org/10.1007/s11104-016-3135-3

Rowley, M. C., Grand, S., & Verrecchia, É. P. (2018). Calcium-mediated stabilisation of soil organic carbon. *Biogeochemistry*, *137*(1–2), 27–49. https://doi.org/10.1007/S10533-017-0410-1

Rowley, M.C., Pena, J., Olaka, L.A., Rozin, A., Bone, S.E., Wiesenberg, G.L.B., Hoppe, G.A., Lisabeth, H., Rieder, C., Dasgupta, S., Nico, P., Vaughan, L., Cailleau, G., Bindschedler., S., (In prep). Inorganic carbon sequestration identified in active oxalate-carbonate pathways associated with agroforestry species (Ficus spp.) in East Africa (Samburu County, Kenya).

Ruiz, N., Ward, D., & Saltz, D. (2002). Calcium oxalate crystals in leaves of Pancratium sickenbergeri: Constitutive or induced defence? *Functional Ecology*, *16*(1), 99–105. https://doi.org/10.1046/j.0269-8463.2001.00594.x

Sahin, N. (2003). Oxalotrophic bacteria. *Research in Microbiology*, *154*(6), 399–407. https://doi.org/10.1016/S0923-2508(03)00112-8

Savage, G., Mason, S., Vanhanen, L., & Busch, J. (2004). Oxalate content of raw and cooked silver beet. *… of the Nutrition Society of New …*, *29*, 26–30.

Savage, G. P., Vanhanen, L., Mason, S. M., & Ross, A. B. (2000). Effect of Cooking on the Soluble and Insoluble Oxalate Content of Some New Zealand Foods. *Journal of Food Composition and Analysis*, *13*(3), 201–206. https://doi.org/10.1006/jfca.2000.0879

Schlesinger, W. H. (1982). Carbon storage in the caliche of arid soils: A case study from arizona. *Soil Science*, *133*(4), 247–255. https://doi.org/10.1097/00010694-198204000-00008

Schlesinger, W. H. (1985). The formation of caliche in soils of the Mojave Desert, California. *Geochimica et Cosmochimica Acta*, *49*(1), 57–66. https://doi.org/10.1016/0016-7037(85)90191-7

Schmitt, A. D., Borrelli, N., Ertlen, D., Gangloff, S., Chabaux, F., & Osterrieth, M. (2018). Stable calcium isotope speciation and calcium oxalate production within beech tree (Fagus sylvatica L.) organs. *Biogeochemistry*, *137*(1–2), 197–217. https://doi.org/10.1007/s10533-017-0411-0

Sebuliba, E., Majaliwa, J. G. M., Isubikalu, P., Turyahabwe, N., Eilu, G., & Ekwamu, A. (2022). Characteristics of shade trees used under Arabica coffee agroforestry systems in Mount Elgon Region, Eastern Uganda. *Agroforestry Systems*, *96*(1), 65–77. https://doi.org/10.1007/s10457-021-00688-6

Shen, Y., Luo, X., Li, H., Guan, Q., & Cheng, L. (2021). Evaluation of a high-performance liquid chromatography method for urinary oxalate determination and investigation regarding the pediatric reference interval of spot urinary oxalate to creatinine ratio for screening of primary hyperoxaluria. *Journal of Clinical Laboratory Analysis*, *35*(8). https://doi.org/10.1002/jcla.23870

Sigma-Aldrich Co. LLC. (2023). *Oxalate Assay Kit: Technical Bulletin*.

Simpson, T. S., Savage, G. P., Robert, S., & Vanhanen, L. P. (2009). Oxalate content of silver beet leaves (Beta vulgaris var. cicla) at different stages of maturation and the effect of cooking with different milk sources. *Journal of Agricultural and Food Chemistry*, *57*(22), 10804–10808. https://doi.org/10.1021/jf902124w

Sokolova, T. A. (2020). Low-Molecular-Weight Organic Acids in Soils: Sources, Composition, Concentrations, and Functions: A Review. *Eurasian Soil Science*, *53*(5), 580–594. https://doi.org/10.1134/S1064229320050154

Starkey, B. J., & Fry, I. D. R. (1993). Comparison of a commercial enzymic kit for urinary oxalate analysis with a high performance liquid chromatographic method. *Annals of Clinical Biochemistry*, *30*(2), 186–190. https://doi.org/10.1177/000456329303000213

Stöckl, D., D'Hondt, H., & Thienpont, L. M. (2009). Method validation across the disciplines-Critical investigation of major validation criteria and associated experimental protocols. In *Journal of Chromatography B: Analytical Technologies in the Biomedical and Life Sciences* (Vol. 877, Issue 23, pp. 2180–2190). Elsevier. https://doi.org/10.1016/j.jchromb.2008.12.056

Strobel, B. W., Kristensen, F., & Hansen, H. C. B. (2004). Oxalate distribution in soils under rhubarb (Rheum rhaponticum). *International Journal of Environmental Analytical Chemistry*, *84*(12), 909–917. https://doi.org/10.1080/0306731042000268134

Tasdelen, M. A., Karagoz, B., Bicak, N., & Yagci, Y. (2008). Phenacylpyridinium oxalate as a novel water-soluble photoinitiator for free radical polymerization. *Polymer Bulletin*, *59*(6), 759–766. https://doi.org/10.1007/s00289-007-0822-5

Tiessen, H., Cuevas, E., & Chacon, P. (1994). The role of soil organic matter in sustaining soil fertility. *Nature*, *371*(6500), 783–785. https://doi.org/10.1038/371783a0

Trinity Biotech PLC. (2013). *Trinity Biotech PLC, - Oxalate kit*.

Van Harskamp, D., Garrelfs, S. F., Oosterveld, M. J. S., Groothoff, J. W., Van Goudoever, J. B., & Schierbeek, H. (2020). Development and Validation of a New Gas Chromatography-Tandem Mass Spectrometry Method for the Measurement of Enrichment of Glyoxylate Metabolism Analytes in Hyperoxaluria Patients Using a Stable Isotope Procedure. *Analytical Chemistry*, *92*(2), 1826–1832. https://doi.org/10.1021/acs.analchem.9b03670

Van Hees, P. A. W., Dahlén, J., Lundström, U. S., Borén, H., & Allard, B. (1999). Determination of low molecular weight organic acids in soil solution by HPLC. *Talanta*, *48*(1), 173–179. https://doi.org/10.1016/S0039-9140(98)00236-7

Varão Moura, A., Aparecido Rosini Silva, A., Domingos Santo da Silva, J., Aleixo Leal Pedroza, L., Bornhorst, J., Stiboller, M., Schwerdtle, T., & Gubert, P. (2022). Determination of ions in Caenorhabditis elegans by ion chromatography. *Journal of Chromatography B: Analytical Technologies in the Biomedical and Life Sciences*, *1204*, 123312. https://doi.org/10.1016/j.jchromb.2022.123312

Verrecchia, E. P. (1990). Litho-diagenetic implications of the calcium oxalate-carbonate biogeochemical cycle in semiarid calcretes, nazareth, israel. *Geomicrobiology Journal*, *8*(2), 87–99. https://doi.org/10.1080/01490459009377882

Verrecchia, E. P., Braissant, O., & Cailleau, G. (2006). The oxalate-carbonate pathway in soil carbon storage: The role of fungi and oxalotrophic bacteria. In *Fungi in Biogeochemical Cycles* (Vol. 9780521845, pp. 289–310). https://doi.org/10.1017/CBO9780511550522.013

Volk, G. M., Lynch-Holm, V. J., Kostman, T. A., Goss, L. J., & Franceschi, V. R. (2002). The role of druse and raphide calcium oxalate crystals in tissue calcium regulation in Pistia stratiotes leaves. *Plant Biology*, *4*(1), 34–45. https://doi.org/10.1055/s-2002-20434

Wahab, F. M., & Armstrong, D. W. (2017). Peak Shapes and Their Measurements: The Need and the Concept Behind Total Peak Shape Analysis. *LCGC North America*, *35*(12), 846–853.

Wiedemeier, D. B., Lang, S. Q., Gierga, M., Abiven, S., Bernasconi, S. M., Früh-Green, G. L., Hajdas, I., Hanke, U. M., Hilf, M. D., McIntyre, C. P., Scheider, M. P. W., Smittenberg, R. H., Wacker, L., Wiesenberg, G. L. B., & Schmidt, M. W. I. (2016). Characterization, quantification and compound-specific isotopic analysis of pyrogenic carbon using benzene polycarboxylic acids (Bpca). *Journal of Visualized Experiments*, *2016*(111), e53922. https://doi.org/10.3791/53922

Wiesenberg, G. L. B., Schwark, L., & Schmidt, M. W. I. (2004). Improved automated extraction and separation procedure for soil lipid analyses. *European Journal of Soil Science*, *55*(2), 349–356. https://doi.org/10.1111/j.1351-0754.2004.00601.x

Wu, C. H., Kuo, C. Y., & Lo, S. L. (2009). Recovery of heavy metals from industrial sludge using various acid extraction approaches. *Water Science and Technology*, *59*(2), 289–293. https://doi.org/10.2166/wst.2009.859

Zamanian, K., Zhou, J., & Kuzyakov, Y. (2021). Soil carbonates: The unaccounted, irrecoverable carbon source. *Geoderma*, *384*, 114817. https://doi.org/10.1016/j.geoderma.2020.114817

Zuo, G., Jiang, X., Liu, H., & Zhang, J. (2010). A novel urinary oxalate determination method via a catalase model compound with oxalate oxidase. *Analytical Methods*, *2*(3), 254–258. https://doi.org/10.1039/b9ay00247b

Appendix

A Kenya field notes

Tab. 15: Field notes of analysed tree species

Date	Tree species and replicate	Circum-ference (m)	Half (2) or not (1)	DBH[1] (m)	Distance for angle (m)	Clinometer angle (°)	Extra height + (m)	Height of observer (m)	Tree height (m)
17.10.2022	*Ficus Glumosa* 1	3.3	2	2.10	49.8	24	0	1.68	23.85
17.10.2022	*Ficus Glumosa* 2	5.5	1	1.75	34	21	0	1.68	14.73
17.10.2022	*Ficus Glumosa* 3	3.9	2	2.48	31.5	25	0	1.68	16.37
17.10.2022	*Ficus Glumosa* 4	2.5	2	1.59	30.2	20	0	1.68	12.67
17.10.2022	*Ficus Glumosa* 5	6.7	1	2.13	33	24	0	1.68	16.37
18.10.2022	*Ficus Natalensis* 1	4.0	2	2.55	41.8	29	0	1.68	24.85
18.10.2022	*Ficus Natalensis* 2	2.9	2	1.85	32	34	0	1.68	23.26
18.10.2022	*Ficus Natalensis* 3	3.3	2	2.10	39.7	32	1	1.68	27.49
18.10.2022	*Ficus Sycomorus* 1	4.91	1	1.56	29.2	14	0	1.68	8.96
18.10.2022	*Ficus Sycomorus* 2	3.83	1	1.22	22.3	16	0	1.68	8.07
18.10.2022	*Ficus Sycomorus* 3	3.75	1	1.19	17.2	22	0	1.68	8.63
18.10.2022	*Ficus Sycomorus* 4	2.7	1	0.86	29.5	9	2	1.68	8.35
18.10.2022	*Ficus Sycomorus* 5	1.89	1	0.60	14	20	0	1.68	6.78

[1] DBH = Diameter at breast height

B Detailed method development steps

Tab. 16: Method development steps of the HPLC method and their corresponding retention times

Date	Sample	Solvent A	Solvent B	Flow rate (mL/min)	Column temperature (°C)	Number of columns	Injection volume (µL)	Wave-length (nm)	Retention time (min)
26.06.2024	70 mg/L standard (std)	85 % 0.17 M CH_3COONH_4	15 % MeOH	1	25	1 x 100 mm	3	216	no peak
26.06.2024	70 mg/L std	85 % 0.17 M CH_3COONH_4	15 % MeOH	1	25	1 x 100 mm	20	216	no peak
26.06.2024	70 mg/L std	99.5 % 20 mM H_3PO_4	0.5 % ACN	1	25	1 x 100 mm	20	216	1.03
26.06.2024	70 mg/L std	99.5 % 20 mM H_3PO_4	0.5 % ACN	1	25	1 x 100 mm	10	216	1.03
26.06.2024	70 mg/L std	99.5 % H_2O	0.5 % ACN	1	25	1 x 100 mm	10	216	no peak
27.06.2024	70 mg/L std	90 % MeOH	10 % ACN	1	25	1 x 100 mm	20	216	0.74
27.06.2024	70 mg/L std	80 % MeOH	20 % ACN	1	25	1 x 100 mm	20	216	0.75
27.06.2024	70 mg/L std	70 % MeOH	30 % ACN	1	25	1 x 100 mm	20	216	0.79

Tab. 16: Cont.

Date	Sample	Solvent A	Solvent B	Flow rate (mL/min)	Column temperature (°C)	Number of columns	Injection volume (µL)	Wave-length (nm)	Retention time (min)
27.06.2024	70 mg/L std	60 % MeOH	40 % ACN	1	25	1 x 100 mm	20	216	0.78
27.06.2024	70 mg/L std	50 % MeOH	50 % ACN	1	25	1 x 100 mm	20	216	0.78
27.06.2024	70 mg/L std	40 % MeOH	60 % ACN	1	25	1 x 100 mm	20	216	0.78
27.06.2024	70 mg/L std	30 % MeOH	70 % ACN	1	25	1 x 100 mm	20	216	0.81
27.06.2024	70 mg/L std	30 % 20 mM H_3PO_4	70 % ACN	0.8	25	1 x 100 mm	20	216	1.00
27.06.2024	70 mg/L std	30 % 20 mM H_3PO_4	70 % ACN	0.6	25	1 x 100 mm	20	216	1.32
27.06.2024	70 mg/L std	70 % 20 mM H_3PO_4	30 % ACN	0.5	25	1 x 100 mm	20	216	1.58
27.06.2024	70 mg/L std.	30 % 20 mM H_3PO_4	70 % ACN	0.5	25	1 x 100 mm	20	216	1.85
27.06.2024	70 mg/L std	30 % 20 mM H_3PO_4	70 % ACN	0.4	25	1 x 100 mm	20	216	2.3

Tab. 16: Cont.

Date	Sample	Solvent A	Solvent B	Flow rate (mL/min)	Column temperature (°C)	Number of columns	Injection volume (µL)	Wave-length (nm)	Retention time (min)
27.06.2024	70 mg/L std	30 % 20 mM H_3PO_4	70 % ACN	0.3	25	1 x 100 mm	20	216	3.07
27.06.2024	70 mg/L std	30 % 20 mM H_3PO_4	70 % ACN	0.2	25	1 x 100 mm	20	216	4.61
27.06.2024	70 mg/L std	20 % 20 mM H_3PO_4	80 % ACN	0.4	25	1 x 100 mm	20	216	2.36
27.06.2024	70 mg/L std	10 % 20 mM H_3PO_4	90 % ACN	0.4	25	1 x 100 mm	20	216	no peak
27.06.2024	35 mg/L std	30 % 20 mM H_3PO_4	70 % ACN	0.4	25	1 x 100 mm	20	216	2.29
27.06.2024	140 mg/L std	30 % 20 mM H_3PO_4	70 % ACN	0.4	25	1 x 100 mm	20	216	2.27
27.06.2024	*F. Glumosa* 3, Bark, pH neut.	30 % 20 mM H_3PO_4	70 % ACN	0.4	25	1 x 100 mm	20	216	several
27.06.2024	*F. Glumosa* 3, Bark, pH 1	30 % 20 mM H_3PO_4	70 % ACN	0.4	25	1 x 100 mm	20	216	several

Tab. 16: Cont.

Date	Sample	Solvent A	Solvent B	Flow rate (mL/min)	Column temperature (°C)	Number of columns	Injection volume (µL)	Wave-length (nm)	Retention time (min)
27.06.2024	*F. Natalensis* 2, Branch, pH 2	30 % 20 mM H_3PO_4	70 % ACN	0.4	25	1 x 100 mm	20	216	several
27.06.2024	*F. Natalensis* 2, Branch, pH 4	30 % 20 mM H_3PO_4	70 % ACN	0.4	25	1 x 100 mm	20	216	several
27.06.2024	140 mg/L std	0.5 % 20 mM H_3PO_4	99.5 % ACN	0.4	25	1 x 100 mm	20	216	no peak
27.06.2024	140 mg/L std	0.5 % 20 mM H_3PO_4	99.5 % ACN	0.4	25	1 x 100 mm	20	216	several
27.06.2024	140 mg/L std	0.5 % 20 mM H_3PO_4	99.5 % ACN	0.4	25	1 x 100 mm	20	**216**, 260, 280	several
27.06.2024	35 mg/L std	30 % 20 mM H_3PO_4	70 % ACN	0.4	25	1 x 100 mm	20	**216**, 260, 280	several

Tab. 16: Cont.

Date	Sample	Solvent A	Solvent B	Flow rate (mL/min)	Column temperature (°C)	Number of columns	Injection volume (µL)	Wave-length (nm)	Retention time (min)
27.06.2024	*F. Glumosa* 3, pH 1	30 % 20 mM H_3PO_4	70 % ACN	0.4	25	1 x 100 mm	20	**216**, 260, 280	several
02.07.2024	70 mg/L std	30 % 400 mM H_3PO_4	70 % ACN	0.4	25	1 x 100 mm	20	**216**, 260, 280	two peaks: 2 (small), 2.31 (large)
02.07.2024	70 mg/L std	30 % 400 mM H_3PO_4	70 % ACN	0.4	25	1 x 100 mm	20	**216**, 260, 280	two peaks: 2 (small), 2.31 (large)
02.07.2024	140 mg/L std	30 % 400 mM H_3PO_4	70 % ACN	0.4	25	1 x 100 mm	20	**216**, 260, 280	two peaks: 2 (small), 2.325 (large)
02.07.2024	70 mg/L std	30 % 400 mM H_3PO_4	70 % ACN	0.4	25	1 x 100 mm	20	**216**, 260, 280	2.32

Tab. 16: Cont.

Date	Sample	Solvent A	Solvent B	Flow rate (mL/min)	Column temperature (°C)	Number of columns	Injection volume (µL)	Wave-length (nm)	Retention time (min)
02.07.2024	140 mg/L std	30 % 400 mM H_3PO_4	70 % ACN	0.4	25	1 x 100 mm	20	**216**, 260, 280	2.32
02.07.2024	70 mg/L std	60 % 400 mM H_3PO_4	40 % ACN	0.4	25	1 x 100 mm	20	**216**, 260, 280	two peaks: 2.31 & 2.39
02.07.2024	140 mg/L std	60 % 400 mM H_3PO_4	40 % ACN	0.4	25	1 x 100 mm	20	**216**, 260, 280	two peaks: 2.31 & 2.38
02.07.2024	70 mg/L std	90 % 400 mM H_3PO_4	10 % ACN	0.4	25	1 x 100 mm	20	**216**, 260, 280	two peaks: 2.343 & 2.59
02.07.2024	140 mg/L std	90 % 400 mM H_3PO_4	10 % ACN	0.4	25	1 x 100 mm	20	**216**, 260, 280	2.590
02.07.2024	140 mg/L std	90 % 400 mM H_3PO_4	10 % ACN	0.4	25	1 x 100 mm	20	**216**, 260, 280	2.60

Tab. 16: Cont.

Date	Sample	Solvent A	Solvent B	Flow rate (mL/min)	Column temperature (°C)	Number of columns	Injection volume (µL)	Wave-length (nm)	Retention time (min)
02.07.2024	140 mg/L std	90 % 400 mM H_3PO_4	10 % ACN	0.4	20	1 x 100 mm	20	**216**, 260, 280	2.61
02.07.2024	140 mg/L std	90 % 400 mM H_3PO_4	10 % ACN	0.4	15	1 x 100 mm	20	**216**, 260, 280	2.63
02.07.2024	*F. Natalensis* 1, Leaf, pH 1	90 % 400 mM H_3PO_4	10 % ACN	0.4	10	1 x 100 mm	20	**216**, 260, 280	2.62
03.07.2024	140 mg/L std	90 % 400 mM H_3PO_4	10 % ACN	0.4	10	1 x 100 mm	20	**216**, 260, 280	2.63
03.07.2024	140 mg/L std	90 % 400 mM H_3PO_4	10 % ACN	0.4	10	1 x 100 mm	20	**216**, 260, 280	2.64
03.07.2024	140 mg/L std	90 % 400 mM H_3PO_4	10 % ACN	0.4	8	1 x 100 mm	20	**216**, 260, 280	2.65

Tab. 16: Cont.

Date	Sample	Solvent A	Solvent B	Flow rate (mL/min)	Column temperature (°C)	Number of columns	Injection volume (µL)	Wave-length (nm)	Retention time (min)
03.07.2024	*F. Sycomorus* 4, Bark	90 % 400 mM H_3PO_4	10 % ACN	0.4	5	1 x 100 mm	20	**216**, 260, 280	2.68
03.07.2024	140 mg/L std	85 % 400 mM H_3PO_4	15 % ACN	0.4	5	1 x 100 mm	20	**216**, 260, 280	2.60
03.07.2024	140 mg/L std	80 % 400 mM H_3PO_4	20 % ACN	0.4	5	1 x 100 mm	20	**216**, 260, 280	2.56
03.07.2024	140 mg/L std	70 % 400 mM H_3PO_4	30 % ACN	0.4	5	1 x 100 mm	20	**216**, 260, 280	2.47
03.07.2024	140 mg/L std	70 % 400 mM H_3PO_4	30 % ACN	0.4	5	1 x 100 mm	20	**216**, 260, 280	2.46
03.07.2024	140 mg/L std	80 % 400 mM H_3PO_4	20 % ACN	0.4	8	1 x 100 mm	20	**216**, 260, 280	2.54

Tab. 16: Cont.

Date	Sample	Solvent A	Solvent B	Flow rate (mL/min)	Column temperature (°C)	Number of columns	Injection volume (µL)	Wave-length (nm)	Retention time (min)
03.07.2024	*F. Sycomorus* 4, Bark	90 % 400 mM H_3PO_4	10 % ACN	0.4	8	1 x 100 mm	20	**216**, 260, 280	2.66
03.07.2024	*F. Natalensis* 2, Root	90 % 400 mM H_3PO_4	10 % ACN	0.4	8	1 x 100 mm	20	**216**, 260, 280	2.63
03.07.2024	*F. Sycomorus* 4, Bark	80 % 400 mM H_3PO_4	20 % ACN	0.4	8	1 x 100 mm	20	**216**, 230, 280	2.65
03.07.2024	*F. Natalensis* 2, Root	80 % 400 mM H_3PO_4	20 % ACN	0.4	8	1 x 100 mm	20	**210**, 230, 280	2.68
03.07.2024	140 mg/L std	95 % 400 mM H_3PO_4	5 % ACN	0.4	8	1 x 100 mm	20	**210**, 230, 280	2.88
03.07.2024	140 mg/L std	95 % 400 mM H_3PO_4	5 % ACN	0.4	8	1 x 100 mm	20	**210**, 230, 280	2.88

Tab. 16: Cont.

Date	Sample	Solvent A	Solvent B	Flow rate (mL/min)	Column temperature (°C)	Number of columns	Injection volume (µL)	Wave-length (nm)	Retention time (min)
03.07.2024	140 mg/L std	99 % 400 mM H_3PO_4	1 % ACN	0.4	8	1 x 100 mm	20	**210**, 230, 280	3.05
03.07.2024	140 mg/L std	99.5 % 400 mM H_3PO_4	0.5 % ACN	0.4	8	1 x 100 mm	20	**210**, 230, 280	3.09
03.07.2024	140 mg/L std	99.5 % 400 mM H_3PO_4	0.5 % ACN	0.4	8	1 x 100 mm	20	**210**, 230, 280	3.10
03.07.2024	*F. Sycomorus* 4, Bark	99.5 % 400 mM H_3PO_4	0.5 % ACN	0.4	8	1 x 100 mm	20	**210**, 230, 280	3.08
04.07.2024	140 mg/L std	99.5 % 400 mM H_3PO_4	0.5 % ACN	0.4	8	1 x 100 mm	20	**210**, 230, 280	3.03
04.07.2024	*F. Sycomorus* 4, Bark	99.5 % 400 mM H_3PO_4	0.5 % ACN	0.4	8	1 x 100 mm	10	**210**, 230, 280	3.03

Tab. 16: Cont.

Date	Sample	Solvent A	Solvent B	Flow rate (mL/min)	Column temperature (°C)	Number of columns	Injection volume (µL)	Wave-length (nm)	Retention time (min)
04.07.2024	*F. Sycomorus* 4, Bark	99.5 % 400 mM H_3PO_4	0.5 % ACN	0.4	8	1 x 100 mm	5	**210**, 230, 280	3.03
04.07.2024	*F. Natalensis* 2, Bark	99.5 % 400 mM H_3PO_4	0.5 % ACN	0.4	8	1 x 100 mm	5	**210**, 230, 280	3.02
04.07.2024	*F. Natalensis* 2, Bark	99.9 % 400 mM H_3PO_4	0.1 % ACN	0.4	8	1 x 100 mm	5	**210**, 230, 280	3.03
04.07.2024	*F. Natalensis* 2, Bark	99.9 % 400 mM H_3PO_4	0.1 % ACN	0.4	8	1 x 100 mm	5	**210**, 230, 280	3.04
04.07.2024	*F. Natalensis* 1, Leaf	99.9 % 400 mM H_3PO_4	0.1 % ACN	0.4	8	1 x 100 mm	5	**210**, 230, 280	3.04
04.07.2024	F. Natalensis 2, Branch	99.9 % 400 mM H_3PO_4	0.1 % ACN	0.4	8	1 x 100 mm	5	**210**, 230, 280	3.07

Tab. 16: Cont.

Date	Sample	Solvent A	Solvent B	Flow rate (mL/min)	Column temperature (°C)	Number of columns	Injection volume (µL)	Wave-length (nm)	Retention time (min)
04.07.2024	*F. Natalensis* 2, Root	99.9 % 400 mM H_3PO_4	0.1 % ACN	0.4	8	1 x 100 mm	5	**210**, 230, 280	3.06
04.07.2024	*F. Glumosa* 3, Bark	99.9 % 400 mM H_3PO_4	0.1 % ACN	0.4	8	1 x 100 mm	5	**210**, 230, 280	no peak, probably empty
04.07.2024	*F. Sycomorus* 4, Bark	99.9 % 20 mM H_3PO_4	0.1 % ACN	0.4	8	1 x 100 mm	5	**210**, 230, 280	2.76
08.07.2024	140 mg/L std	99.9 % 400 mM H_3PO_4	0.1 % ACN	0.4	8	2 x 100 mm	20	**210**, 230, 280	6.1
08.07.2024	140 mg/L std	99.9 % 400 mM H_3PO_4	0.1 % ACN	0.4	8	2 x 100 mm	20	**210**, 230, 280	6.1
08.07.2024	*F. Natalensis* 2, Bark	99.9 % 400 mM H_3PO_4	0.1 % ACN	0.4	8	2 x 100 mm	5	**210**, 230, 280	6.09

Tab. 16: Cont.

Date	Sample	Solvent A	Solvent B	Flow rate (mL/min)	Column temperature (°C)	Number of columns	Injection volume (µL)	Wave-length (nm)	Retention time (min)
08.07.2024	*F. Glumosa* 3, Bark	99.9 % 400 mM H_3PO_4	0.1 % ACN	0.4	8	2 x 100 mm	5	**210**, 230, 280	6.12
08.07.2024	*F. Natalensis* 2, Bark	99.9 % 400 mM H_3PO_4	0.1 % ACN	0.4	8	2 x 100 mm	5	**210**, 230, 280	6.10
23.07.2024	140 mg/L standard	99.9 % 400 mM H_3PO_4	0.1 % ACN	0.4	8	2 x 100 mm	5	**210**, 230, 280	6.09
23.07.2024	*F. Natalensis* 2, Bark	99.9 % 400 mM H_3PO_4	0.1 % ACN	0.4	8	2 x 100 mm	5	**210**, 230, 280	6.09
24.07.2024	*F. Natalensis* 2, Bark	99.9 % 400 mM H_3PO_4	0.1 % ACN	0.4	8	2 x 100 mm	5	**210**, 230, 280	6.08
24.07.2024	*F. Natalensis* 2, Bark	99.9 % 400 mM H_3PO_4	0.1 % ACN	0.4	8	2 x 100 mm	5	**210**, 230, 280	6.10

Tab. 16: Cont.

Date	Sample	Solvent A	Solvent B	Flow rate (mL/min)	Column temperature (°C)	Number of columns	Injection volume (µL)	Wave-length (nm)	Retention time (min)
24.07.2024	*F. Natalensis* 2, Bark	99.9 % 400 mM H_3PO_4	0.1 % ACN	0.4	8	2 x 100 mm	5	**210**, 230, 280	6.09
25.07.2024	140 mg/L std	99.9 % 400 mM H_3PO_4	0.1 % ACN	0.4	8	2 x 100 mm	5	**210**, 230, 280	6.09
30.07.2024	140 mg/L std	99.9 % 400 mM H_3PO_4	0.1 % ACN:H_2O (1:1)	0.4	8	2 x 150 mm	20	200, **210**, 230, 280	8.89
09.08.2024	*F. Glumosa* 5, Litter	99.9 % 400 mM H_3PO_4	0.1 % ACN:H_2O (1:1)	0.4	8	2 x 150 mm	5	200, **210**, 230, 280	8.91
09.08.2024	*F. Glumosa* 2, Adjacent	99.9 % 400 mM H_3PO_4	0.1 % ACN:H_2O (1:1)	0.4	8	2 x 150 mm	10	200, **210**, 230, 280	8.90

Tab. 16: Cont.

Date	Sample	Solvent A	Solvent B	Flow rate (mL/min)	Column temperature (°C)	Number of columns	Injection volume (µL)	Wave-length (nm)	Retention time (min)
09.08.2024	*F. Glumosa* 2, Adjacent	99.9 % 400 mM H_3PO_4	0.1 % ACN:H_2O (1:1)	0.4	8	3 x 150 mm	10	200, **210**, 230, 280	13.02
09.08.2024	*F. Glumosa* 5, Litter	99.9 % 400 mM H_3PO_4	0.1 % ACN:H_2O (1:1)	0.4	8	3 x 150 mm	5	200, **210**, 230, 280	12.97
13.08.2024	*F. Glumosa* 2, Adjacent	99.9 % 400 mM H_3PO_4	0.1 % ACN:H_2O (1:1)	0.4	8	2 x 150 mm	10	200, **210**, 230, 280	8.99
13.08.2024	*F. Glumosa* 2, Adjacent	99.9 % 400 mM H_3PO_4	0.1 % ACN:H_2O (1:1)	0.4	8	2 x 150 mm	10	200, **210**, 230, 280	9.01

C CaOx contents obtained during method validation

Tab. 17: CaOx contents of organic matter samples

Date of measurement	Sample	CaOx content (g/kg)	CaOx content (%)
08.10.2024	*F. Glumosa* 1, Leaf	7.04	0.70
28.10.2024	*F. Glumosa* 1, Litter	40.59	4.06
08.10.2024	*F. Glumosa* 1, Branch	39.09	3.91
08.10.2024	*F. Glumosa* 1, Root	126.71	12.67
08.10.2024	*F. Glumosa* 1, Bark	52.59	5.26
08.10.2024	*F. Glumosa* 2, Leaf	11.33	1.13
08.10.2024	*F. Glumosa* 2, Litter	28.28	2.83
08.10.2024	*F. Glumosa* 2, Branch	55.89	5.59
08.10.2024	*F. Glumosa* 2, Root	40.72	4.07
08.10.2024	*F. Glumosa* 2, Bark	30.76	3.08
08.10.2024	*F. Glumosa* 3, Leaf	23.11	2.31
28.10.2024	*F. Glumosa* 3, Litter	60.84	6.08
08.10.2024	*F. Glumosa* 3, Branch	37.50	3.75
08.10.2024	*F. Glumosa* 3, Root	72.19	7.22
08.10.2024	*F. Glumosa* 3, Bark	74.39	7.44
08.10.2024	*F. Glumosa* 4, Leaf	1.94	0.19
08.10.2024	*F. Glumosa* 4, Litter	2.64	0.26
08.10.2024	*F. Glumosa* 4, Branch	4.33	0.43
08.10.2024	*F. Glumosa* 4, Root	65.46	6.55
08.10.2024	*F. Glumosa* 4, Bark	46.51	4.65
08.10.2024	*F. Glumosa* 5, Leaf	12.88	1.29
08.10.2024	*F. Glumosa* 5, Litter	25.96	2.60
22.10.2024	*F. Glumosa* 5, Branch	143.99	14.40
22.10.2024	*F. Glumosa* 5, Root	92.93	9.29
22.10.2024	*F. Glumosa* 5, Bark	72.54	7.25
28.10.2024	*F. Natalensis* 1, Leaf	64.74	6.47
22.10.2024	*F. Natalensis* 1, Litter	95.22	9.52
22.10.2024	*F. Natalensis* 1, Branch	76.73	7.67
22.10.2024	*F. Natalensis* 1, Root	160.69	16.07
22.10.2024	*F. Natalensis* 1, Bark	31.80	3.18
22.10.2024	*F. Natalensis* 2, Leaf	112.75	11.27
22.10.2024	*F. Natalensis* 2, Litter	155.62	15.56
22.10.2024	*F. Natalensis* 2, Branch	101.66	10.17
22.10.2024	*F. Natalensis* 2, Root	80.55	8.06
22.10.2024	*F. Natalensis* 2, Bark	102.11	10.21
22.10.2024	*F. Natalensis* 3, Leaf	65.63	6.56
22.10.2024	*F. Natalensis* 3, Litter	61.61	6.16
22.10.2024	*F. Natalensis* 3, Branch	146.35	14.63
22.10.2024	*F. Natalensis* 3, Root	129.44	12.94
22.10.2024	*F. Natalensis* 3, Bark	60.82	6.08
22.10.2024	*F. Sycomorus* 1, Leaf	22.26	2.23
22.10.2024	*F. Sycomorus* 1, Litter	37.59	3.76
22.10.2024	*F. Sycomorus* 1, Branch	38.24	3.82

Tab. 17: Cont.

Date of measurement	Sample	CaOx content (g/kg)	CaOx content (%)
22.10.2024	*F. Sycomorus* 1, Root	29.87	2.99
22.10.2024	*F. Sycomorus* 1, Bark	168.89	16.89
28.10.2024	*F. Sycomorus* 2, Leaf	25.27	2.53
28.10.2024	*F. Sycomorus* 2, Litter	45.79	4.58
28.10.2024	*F. Sycomorus* 2, Branch	25.96	2.60
28.10.2024	*F. Sycomorus* 2, Root	163.32	16.33
28.10.2024	*F. Sycomorus* 2, Bark	130.20	13.02
28.10.2024	*F. Sycomorus* 3, Leaf	17.34	1.73
28.10.2024	*F. Sycomorus* 3, Litter	41.90	4.19
28.10.2024	*F. Sycomorus* 3, Branch	61.89	6.19
28.10.2024	*F. Sycomorus* 3, Root	109.67	10.97
28.10.2024	*F. Sycomorus* 3, Bark	182.85	18.28
28.10.2024	*F. Sycomorus* 4, Leaf	26.50	2.65
28.10.2024	*F. Sycomorus* 4, Litter	25.01	2.50
28.10.2024	*F. Sycomorus* 4, Branch	12.79	1.28
28.10.2024	*F. Sycomorus* 4, Root	165.94	16.59
28.10.2024	*F. Sycomorus* 4, Bark	119.80	11.98
28.10.2024	*F. Sycomorus* 5, Leaf	19.32	1.93
28.10.2024	*F. Sycomorus* 5, Litter	14.97	1.50
28.10.2024	*F. Sycomorus* 5, Branch	58.94	5.89
28.10.2024	*F. Sycomorus* 5, Root	119.53	11.95
28.10.2024	*F. Sycomorus* 5, Bark	45.24	4.52
30.10.2024	*F. Glumosa* 1, Bark, Replicate	62.96	6.30
30.10.2024	*F. Glumosa* 3, Root, Replicate	131.33	13.13
30.10.2024	*F. Glumosa* 4, Leaf, Replicate	3.45	0.35
30.10.2024	*F. Natalensis* 2, Bark, Replicate	45.34	4.53
30.10.2024	*F. Natalensis* 3, Branch, Replicate	152.86	15.29
30.10.2024	*F. Sycomorus* 1, Leaf, Replicate	22.26	2.23
30.10.2024	*F. Sycomorus* 4, Litter, Replicate	22.78	2.28
30.10.2024	*F. Sycomorus* 5, Branch, Replicate	66.88	6.69

Tab. 18: CaOx contents of soil samples

Date of measurement	Sample	CaOx content (g/kg)	CaOx content (%)
18.09.2024	*F. Glumosa* 1, Adjacent	6.52	0.65
18.09.2024	*F. Glumosa* 1, 1 m	2.89	0.29
18.09.2024	*F. Glumosa* 1, 2 m	4.61	0.46
18.09.2024	*F. Glumosa* 1, 3 m	5.64	0.56
18.09.2024	*F. Glumosa* 1, Control	2.73	0.27
18.09.2024	*F. Glumosa* 2, Adjacent	1.89	0.19
18.09.2024	*F. Glumosa* 2, 1 m	1.14	0.11
18.09.2024	*F. Glumosa* 2, 2 m	0.55	0.06
18.09.2024	*F. Glumosa* 2, 3 m	1.05	0.10
18.09.2024	*F. Glumosa* 2, Control	0.35	0.03
18.09.2024	*F. Glumosa* 3, Adjacent	2.06	0.21
18.09.2024	*F. Glumosa* 3, 1 m	2.40	0.24
18.09.2024	*F. Glumosa* 3, 2 m	5.11	0.51
18.09.2024	*F. Glumosa* 3, 3 m	5.43	0.54
18.09.2024	*F. Glumosa* 3, Control	0.36	0.04
23.09.2024	*F. Glumosa* 4, Adjacent	3.65	0.36
23.09.2024	*F. Glumosa* 4, 1 m	0.51	0.05
23.09.2024	*F. Glumosa* 4, 2 m	0.61	0.06
23.09.2024	*F. Glumosa* 4, 3 m	0.53	0.05
23.09.2024	*F. Glumosa* 4, Control	0.14	0.01
23.09.2024	*F. Glumosa* 5, Adjacent	1.70	0.17
23.09.2024	*F. Glumosa* 5, 1 m	1.84	0.18
23.09.2024	*F. Glumosa* 5, 2 m	1.88	0.19
23.09.2024	*F. Glumosa* 5, 3 m	0.89	0.09
23.09.2024	*F. Glumosa* 5, Control	0.35	0.03
11.09.2024	*F. Glumosa*, Adjacent Profile 1	5.53	0.55
18.09.2024	*F. Glumosa*, Adjacent Profile 2	4.63	0.46
11.09.2024	*F. Glumosa*, Adjacent Profile 3	3.17	0.32
18.09.2024	*F. Glumosa*, Adjacent Profile 4	1.67	0.17
11.09.2024	*F. Glumosa*, Adjacent Profile 5	2.70	0.27
11.09.2024	*F. Glumosa*, Control Profile 1	0.16	0.02
18.09.2024	*F. Glumosa*, Control Profile 2	0.20	0.02
11.09.2024	*F. Glumosa*, Control Profile 3	0.30	0.03
18.09.2024	*F. Glumosa*, Control Profile 4	0.43	0.04
11.09.2024	*F. Glumosa*, Control Profile 5	0.58	0.06

Tab. 18: Cont.

Date of measurement	Sample	CaOx content (g/kg)	CaOx content (%)
23.09.2024	*F. Natalensis* 1, Adjacent	3.47	0.35
23.09.2024	*F. Natalensis* 1, 1 m	4.17	0.42
23.09.2024	*F. Natalensis* 1, 2 m	2.75	0.28
23.09.2024	*F. Natalensis* 1, 3 m	2.60	0.26
23.09.2024	*F. Natalensis* 1, Control	0.50	0.05
23.09.2024	*F. Natalensis* 2, Adjacent	9.20	0.92
23.09.2024	*F. Natalensis* 2, 1 m	3.56	0.36
23.09.2024	*F. Natalensis* 2, 2 m	2.39	0.24
23.09.2024	*F. Natalensis* 2, 3 m	3.42	0.34
23.09.2024	*F. Natalensis* 2, Control	1.58	0.16
25.09.2024	*F. Natalensis* 3, Adjacent	3.36	0.34
25.09.2024	*F. Natalensis* 3, 1 m	1.31	0.13
25.09.2024	*F. Natalensis* 3, 2 m	0.78	0.08
25.09.2024	*F. Natalensis* 3, 3 m	0.75	0.08
25.09.2024	*F. Natalensis* 3, Control	0.45	0.04
11.09.2024	*F. Natalensis*, Adjacent Profile 1	0.76	0.08
25.09.2024	*F. Natalensis*, Adjacent Profile 2	0.47	0.05
11.09.2024	*F. Natalensis*, Adjacent Profile 3	3.69	0.37
25.09.2024	*F. Natalensis*, Adjacent Profile 4	0.69	0.07
11.09.2024	*F. Natalensis*, Adjacent Profile 5	4.76	0.48
11.09.2024	*F. Natalensis*, Control Profile 1	2.86	0.29
25.09.2024	*F. Natalensis*, Control Profile 2	2.40	0.24
11.09.2024	*F. Natalensis*, Control Profile 3	1.45	0.15
25.09.2024	*F. Natalensis*, Control Profile 4	2.65	0.26
11.09.2024	*F. Natalensis*, Control Profile 5	1.41	0.14
25.09.2024	*F. Sycomorus* 1, Adjacent	0.87	0.09
25.09.2024	*F. Sycomorus* 1, 1 m	0.59	0.06
25.09.2024	*F. Sycomorus* 1, 2 m	0.86	0.09
25.09.2024	*F. Sycomorus* 1, 3 m	0.51	0.05
25.09.2024	*F. Sycomorus* 1, Control	0.46	0.05
25.09.2024	*F. Sycomorus* 2, Adjacent	1.72	0.17
25.09.2024	*F. Sycomorus* 2, 1 m	1.38	0.14
25.09.2024	*F. Sycomorus* 2, 2 m	0.43	0.04
25.09.2024	*F. Sycomorus* 2, 3 m	0.44	0.04
25.09.2024	*F. Sycomorus* 2, Control	0.17	0.02

Tab. 18: Cont.

Date of measurement	Sample	CaOx content (g/kg)	CaOx content (%)
30.09.2024	*F. Sycomorus* 3, Adjacent	0.95	0.09
30.09.2024	*F. Sycomorus* 3, 1 m	2.32	0.23
30.09.2024	*F. Sycomorus* 3, 2 m	0.60	0.06
30.09.2024	*F. Sycomorus* 3, 3 m	0.29	0.03
30.09.2024	*F. Sycomorus* 3, Control	0.24	0.02
30.09.2024	*F. Sycomorus* 4, Adjacent	0.98	0.10
30.09.2024	*F. Sycomorus* 4, 1 m	1.49	0.15
30.09.2024	*F. Sycomorus* 4, 2 m	1.41	0.14
30.09.2024	*F. Sycomorus* 4, 3 m	0.87	0.09
30.09.2024	*F. Sycomorus* 4, Control	0.23	0.02
30.09.2024	*F. Sycomorus* 5, Adjacent	0.46	0.05
30.09.2024	*F. Sycomorus* 5, 1 m	0.82	0.08
30.09.2024	*F. Sycomorus* 5, 2 m	0.40	0.04
30.09.2024	*F. Sycomorus* 5, 3 m	0.30	0.03
30.09.2024	*F. Sycomorus* 5, Control	0.16	0.02
11.09.2024	*F. Sycomorus*, Adjacent Profile 1	2.43	0.24
11.09.2024	*F. Sycomorus*, Adjacent Profile 2	1.62	0.16
11.09.2024	*F. Sycomorus*, Adjacent Profile 3	1.60	0.16
11.09.2024	*F. Sycomorus*, Adjacent Profile 4	2.06	0.21
11.09.2024	*F. Sycomorus*, Adjacent Profile 5	1.43	0.14
11.09.2024	*F. Sycomorus*, Control Profile 1	0.25	0.02
11.09.2024	*F. Sycomorus*, Control Profile 2	0.25	0.02
11.09.2024	*F. Sycomorus*, Control Profile 3	0.33	0.03
11.09.2024	*F. Sycomorus*, Control Profile 4	0.29	0.03
11.09.2024	*F. Sycomorus*, Control Profile 5	0.18	0.02
30.10.2024	*F. Glumosa*, Adjacent Profile 2, Replicate	4.23	0.42
30.10.2024	*F. Glumosa* 2, Adjacent, Replicate	1.56	0.16
30.10.2024	*F. Glumosa* 3, 1m, Replicate	2.24	0.22
30.10.2024	*F. Glumosa* 4, Control, Replicate	0.10	0.010
30.10.2024	F. Natalensis, Control Profile 4, Replicate	5.28	0.53

Tab. 18: Cont.

Date of measurement	Sample	CaOx content (g/kg)	CaOx content (%)
30.10.2024	*F. Natalensis* 2, Adjacent, Replicate	15.55	1.56
30.10.2024	*F. Natalensis* 3, 2m, Replicate	1.14	0.11
30.10.2024	*F. Sycomorus* 1, Adjacent, Replicate	1.24	0.12
30.10.2024	*F. Sycomorus* 2, 1m, Replicate	2.23	0.22
30.10.2024	*F. Sycomorus* 3, 2m, Replicate	0.79	0.079
30.10.2024	*F. Sycomorus* 4, 3m, Replicate	1.26	0.13
30.10.2024	*F. Sycomorus* 5, Control, Replicate	0.18	0.018

Personal declaration

I hereby declare that the submitted thesis is the result of my own, independent work. All external sources are explicitly acknowledged in the thesis.

Location, date: Signature:

Kloten, 23.04.2025

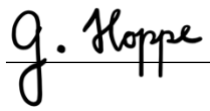

Grittje Hoppe